

A Contrastive Approach to Online Change Point Detection

Artur Goldman, Nikita Puchkin, Valeriia Shcherbakova, and Uliana Vinogradova

Abstract

We suggest a novel procedure for online change point detection. Our approach expands an idea of maximizing a discrepancy measure between points from pre-change and post-change distributions. This leads to flexible algorithms suitable for both parametric and nonparametric scenarios. We prove non-asymptotic bounds on the average running length of the procedure and its expected detection delay. The efficiency of the algorithm is illustrated with numerical experiments on synthetic and real-world data sets.

Index Terms

Sequential change detection, noise-contrastive approach, non-asymptotic bounds, VC class, online convex optimization, follow the approximate leader.

I. INTRODUCTION

THE problem of change point detection is familiar to statisticians and machine learners since the pioneering works of Page [43, 44], Shiryaev [53, 54] and Roberts [49] but, nevertheless, it still attracts attention of many researchers due to its practical importance. In our paper, we assume that a learner observes independent random elements X_1, \dots, X_t, \dots arriving successively. There exists a moment $\tau^* \in \mathbb{N}$ (not accessible to the statistician), such that X_1, \dots, X_{τ^*} are drawn from a distribution, which has a density p with respect to a dominating measure m , while $X_{\tau^*+1}, \dots, X_t, \dots$ have a density q (with respect to the same measure), which differs from p . The measure m is not restricted to be the Lebesgue measure, it can be equal to the counting measure (in the discrete case) or the Hausdorff measure on a low-dimensional manifold as well. The learner is interested in reporting about the occurrence of τ^* as fast as possible while keeping the false alarm rate at an acceptable level. This problem is called online (also referred to as sequential or quickest) change point detection. Such a setup is quite different from another major research direction, offline change point detection [13, 66, 42, 10, 4, 33, 18, 1, 40, 9, 39], where the statistician has an access to the whole time series at once, and, instead of taking decisions on the fly, he is mostly interested in a retrospective analysis and change point localization.

The complexity of a change point detection problem severely depends on the data generating mechanism. The most popular one is a mean shift, that is, $\mathbb{E}X_{\tau^*} \neq \mathbb{E}X_{\tau^*+1}$. Plenty of papers are devoted to a mean shift detection in a univariate or multivariate Gaussian sequence (see, for instance, [15, 45, 48, 7, 56]), but the recent research [14, 61, 65, 64] also considers a more general sub-Gaussian noise. One usually exploits CUSUM-type or likelihood-ratio-type test statistics to perform this task. A broader problem of parametric change point detection (see, for example, [5, 12, 65, 9, 56, 58]) admits that p and q belong to a parametric family of densities $\mathcal{P} = \{p_\theta : \theta \in \Theta\}$. In this setup, the distribution change detection is reduced to detection of a shift in the underlying parameter $\theta \in \Theta$. Both the mean shift model and the parametric change point detection require strong modelling assumptions which are likely to be violated in practical applications. In our paper, we are mostly interested in a nonparametric change point detection problem [27, 23, 66, 36, 4, 18, 1, 34, 41, 52, 16]. We do not impose restrictive conditions on the densities p and q . However, the procedure we propose is quite universal in a sense that it is suitable for different setups, including, for instance, the nonparametric one and the mean shift detection in a multivariate Gaussian sequence model.

Though the number of papers on change point detection is huge and many of them are devoted to theoretical analysis of the procedures (see, e.g., [46, 57, 36, 5, 64, 37, 7, 8, 11, 52]), nonparametric change point detection is studied not so well. Some papers provide rigorous guarantees on the average running length of the procedures (i.e. the expected number of iterations the algorithm makes in a stationary regime until a false alarm) but, to our knowledge, there are no non-asymptotic high probability bounds on the detection delay.

Let us describe the idea of our algorithm. In the sequential change point detection, at the moment t , one usually tests the hypothesis

$$H_0 : X_1, \dots, X_t \text{ have the same distribution} \quad (1)$$

against the composite alternative

$$H_1 : \text{there exists } \tau \in \{1, \dots, t-1\}, \text{ such that } \tau^* = \tau, \quad (2)$$

The preliminary version of this paper [47] was presented at the 26th International Conference on Artificial Intelligence and Statistics (AISTATS), 2023. A. Goldman, V. Shcherbakova, and U. Vinogradova are with HSE University, Moscow, Russian Federation. N. Puchkin is with HSE University and the Institute for Information Transmission Problems RAS, Moscow, Russian Federation, e-mail: npuchkin@hse.ru.

which can be considered as the union of the alternatives of the form $H_1^\tau : \tau^* = \tau$, $\tau \in \{1, \dots, t-1\}$. If the change occurred at some $\tau \in \{1, \dots, t-1\}$ (that is, H_1^τ takes place), then the distribution of X_1, \dots, X_τ must differ from the one of $X_{\tau+1}, \dots, X_t$. To detect such a discrepancy, we introduce an auxiliary function $D : \mathcal{X} \rightarrow (0, 1)$ that should distinguish between the pre-change and post-change distributions. The higher values of $D(X)$ reflect a larger confidence that X was drawn from the density p , rather than from q . Such an approach of reducing an unsupervised learning problem to a supervised one is not new (see, e.g., [24, Section 14.2.4]) and was used in the problems of density estimation [21], generative modelling [19, 20], and density ratio estimation [20]. Based on this idea, Hushchyn, Arzymatov, and Derkach designed an algorithm for change point detection. However, the sliding window technique the authors used leads to significant detection delays. Besides, Hushchyn, Arzymatov, and Derkach do not provide any theoretical guarantees on the running length and the detection delay of their procedure.

Let us fix $t \in \mathbb{N}$ and a change point candidate $\tau \in \{1, \dots, t-1\}$. In order to find a good auxiliary classifier D , distinguishing between X_1, \dots, X_τ and $X_{\tau+1}, \dots, X_t$, we fix a family \mathcal{D} of functions taking their values in $(0, 1)$ and choose a maximizer of the cross-entropy

$$\frac{\tau(t-\tau)}{t} \left[\frac{1}{\tau} \sum_{s=1}^{\tau} \ln(2D(X_s)) + \frac{1}{t-\tau} \sum_{s=\tau+1}^t \ln(2-2D(X_s)) \right] \quad (3)$$

over \mathcal{D} . A similar approach was introduced in [21, 19] but for the purposes of density estimation and generative modelling, respectively. In the context of sequential change point detection, Li, Xie, Dai, and Song [36], as well as Chang, Li, Yang, and Póczos [6], used a different divergence measure, the squared maximum mean discrepancy, to derive a kernel change point detection method. In our paper, we adapt the technique of [19] for the quickest change point detection. Following [21, 19], we call our approach *contrastive* and refer to the function D as discriminator.

We show in Section II-A that our algorithm needs to approximate $\ln(p/q)$ with a reasonable accuracy to be sensitive to distribution changes. This makes it similar to change point detection methods based on the density ratio estimation [38, 29, 28]. For instance, Liu, Yamada, Collier, and Sugiyama use KLIEP [55], uLSIF [30] and RuLSIF [63] for online change point detection. In [28], the authors use the α -relative chi-squared divergence, the same functional as in RuLSIF [63], to construct a change point detection procedure. The advantage of such methods is that the estimation of the ratio p/q can be a much easier task than estimation of the densities p and q themselves. However, in the density-ratio based algorithms the authors usually use a sliding window technique and compare the distributions between two large non-overlapping segments of the time series. This approach shows a good performance in the offline setup, when the learner is interested in change point estimation, but leads to large detection delays in the online case. In our paper, we adjust the test statistic in order to make it suitable for the sequential detection problem. Besides, in contrast to [38, 29, 28], we study the detection delay of our procedure and the behaviour of the test statistic under the null hypothesis.

Contribution. We suggest a procedure for sequential change point detection based on the contrastive approach. We provide non-asymptotic large deviation bounds on the running length and the detection delay of our procedure (Theorems II.8 and II.10) for general classes of discriminators. We also specify the results of these theorems for particular cases, including nonparametric change point detection via neural networks. To our knowledge, Corollary III.1 is the first theoretical guarantee for such a setup. Finally, we illustrate the performance of our procedure with numerical experiments on synthetic and real-world data sets.

Organization of the paper. The rest of the paper is organized as follows. In Section II, we introduce our algorithm and discuss its theoretical properties. In particular, we derive non-asymptotic large deviation bounds on the running length and the detection delay of our procedure (Theorems II.8 and II.10). In Section III, we specify the result of Theorem II.8 for the case when $\ln(p/q)$ is a smooth function. We also show how the result of Theorem II.10 yields an almost optimal mean shift detection in a Gaussian sequence model. In Section II-A, we propose a modified version of the contrastive change point detection method, FALCON, based on tools from online convex optimization. Section V is devoted to numerical experiments. Section VI collects the proofs of our main results, presented in Sections II and III. Some auxiliary results are deferred to appendices.

Notation. We use the following notations throughout the paper. The notation $f \lesssim g$ or $g \gtrsim f$ means that $f \leq cg$ for an absolute constant c . We also use the standard $O(\cdot)$ notation. To avoid problems with the logarithmic function, we use the convention $\log x = (1 \vee \ln x)$. We set $a \wedge b = \min\{a, b\}$, $a \vee b = \max\{a, b\}$, and $a_+ = \max\{a, 0\}$. For $s \geq 1$ and a measure with the density p , we define the $L_s(p)$ -norm as $\|f\|_{L_s(p)} = (\mathbb{E}_{\xi \sim p} |f(\xi)|^s)^{1/s}$, $L_\infty(p)$ -norm as $\|f\|_{L_\infty(p)} = \text{esssup}|f(\xi)|$, where $\xi \sim p$, and the $\psi_s(p)$ -norm as $\|f\|_{\psi_s(p)} = \inf\{u > 0 : \mathbb{E}_{\xi \sim p} \exp(|f(\xi)|^s/u^s) \leq 2\}$. We use the notation $\psi_s(p)$ for the Orlicz norm, instead of the conventional ψ_s , to specify a probability measure and avoid ambiguity, since we deal with different pre-change and post-change distributions. For a class of functions \mathcal{F} , equipped with a norm $\|\cdot\|$, we denote its diameter (with respect to $\|\cdot\|$) by $\mathcal{D}(\mathcal{F}, \|\cdot\|)$. Given two probability measures with the densities $p \ll q$, $\text{KL}(p, q) = \int p(x) \ln(p(x)/q(x)) dx$ stands for the Kullback-Leibler divergence between p and q . For any two densities p and q , $\text{JS}(p, q) = \text{KL}(p, (p+q)/2)/2 + \text{KL}(q, (p+q)/2)/2$ denotes the Jensen-Shannon divergence between p and q .

II. THE ALGORITHM AND ITS THEORETICAL PROPERTIES

In this section, we present our procedure, given in Algorithm II.1, and then discuss its theoretical properties. On each iteration $t \in \mathbb{N}$ and for each change point candidate $\tau \in \{1, \dots, t-1\}$, the algorithm tries to maximize the discrepancy measure (3). The requirement that the classifier D in (3) must take its values in $(0, 1)$ is inconvenient in practical tasks. To avoid this issue, we use the standard reparametrization $D(x) = e^{f(x)}/(1 + e^{f(x)})$, $f \in \mathcal{F}$, obtain the functional $\mathcal{T}_{\tau,t}(f)$ of the form (4) and find its maximizer $\hat{f}_{\tau,t}$. After that, we compute a test statistic \mathcal{S}_t as the maximum of $\mathcal{T}_{\tau,t}(\hat{f}_{\tau,t})$ with respect to τ .

Algorithm II.1 (Contrastive online change point detection).

- **Input:** a class of functions \mathcal{F} and a threshold $\mathfrak{z} > 0$.
- **For** $t = 1, 2, \dots$ **do** the following.
 - 1) Receive an observation X_t .
 - 2) For each $\tau \in \{1, \dots, t-1\}$, compute the estimates $\hat{f}_{\tau,t} \in \operatorname{argmax}_{f \in \mathcal{F}} \mathcal{T}_{\tau,t}(f)$, where

$$\mathcal{T}_{\tau,t}(f) = \frac{t-\tau}{t} \sum_{s=1}^{\tau} \left[f(X_s) - \ln \left(\frac{1 + e^{f(X_s)}}{2} \right) \right] - \frac{\tau}{t} \sum_{s=\tau+1}^t \ln \left(\frac{1 + e^{f(X_s)}}{2} \right). \quad (4)$$

- 3) Compute the test statistic

$$\mathcal{S}_t = \max_{1 \leq \tau \leq t-1} \mathcal{T}_{\tau,t}(\hat{f}_{\tau,t}). \quad (5)$$

- 4) If $\mathcal{S}_t > \mathfrak{z}$, terminate the procedure, and report the change point occurrence.

- **Return.**

At the round t , Algorithm II.1 solves $t-1$ optimization problems. If the class \mathcal{F} is convex, then, using the standard gradient ascent, one can find an ε -maximizer of the functional $\mathcal{T}_{\tau,t}(f)$ in just $O(\log(1/\varepsilon))$ iterations, because of the strong convexity of $\mathcal{T}_{\tau,t}$. Unfortunately, it requires $O(t)$ operations to compute the gradient of $\mathcal{T}_{\tau,t}(f)$. As an alternative, one may use the stochastic gradient ascent to reduce the computational cost of the gradient to $O(1)$. However, such an improvement is not for free, since the stochastic gradient algorithm requires $O(1/\varepsilon)$ iterations to get an ε -maximizer. To sum up, for any $\varepsilon \in (0, 1)$, the procedure requires $O(t^2 \log(1/\varepsilon) \wedge t/\varepsilon)$ operations to compute \mathcal{S}_t within the accuracy ε . This may become prohibitive with the growth of t , and we suggest restarting the procedure from time to time. The good news is that the changes one needs to detect are quite steep in many real-life scenarios, so one does not have to take ε too small nor the class \mathcal{F} too broad. We show in Section V that it is enough to take a class \mathcal{F} of simple structure for consistent change point detection.

A. Behaviour of the test statistic in the presence of a change point

We start with an analysis of the behaviour of the statistic $\mathcal{T}_{\tau,t}(f)$ in the presence of a change point.

Lemma II.2. Fix $t \in \mathbb{N}$ and let $f^*(x) = \ln(p(x)/q(x))$. Assume that the change point occurred at some $\tau \in \{1, 2, \dots, t-1\}$, that is, $\tau^* = \tau$. Then, for any measurable function f , it holds that

$$\mathbb{E} \mathcal{T}_{\tau,t}(f) \geq \frac{2\tau(t-\tau)}{t} \left(\text{JS}(p, q) - \frac{1}{16} \|f - f^*\|_{L_2(p+q)}^2 \right), \quad (6)$$

where $\text{JS}(p, q)$ is the Jensen-Shannon divergence between p and q .

Lemma II.2 illustrates two important properties of $\mathcal{T}_{\tau,t}(f)$. First, if a change point occurred, then, for any $f \in \mathcal{F}$ the expectation of $\mathcal{T}_{\tau^*,t}(f)$ (and, as consequence, the expectation of \mathcal{S}_t) grows as the detection delay $(t - \tau^*)$ increases. We show in the proofs of Theorems II.8 and II.10 that the actual value of \mathcal{S}_t will not be much smaller than its expectation with high probability due to the concentration of measure phenomenon. On the other hand, Lemma II.2 reveals a relation of our procedure with change point detection methods based on density ratio estimation. As one can conclude from (6), the class \mathcal{F} must be chosen in a way to approximate $\ln(p(x)/q(x))$ with a reasonable accuracy. At the same time, as a reader will see in the next section, a broader class \mathcal{F} yields larger values of the test statistics under the null hypothesis. A practitioner must keep this trade-off in mind while choosing \mathcal{F} .

B. Behaviour of the test statistic under the null hypothesis

In this section, we study the behaviour of the test statistic $\mathcal{T}_{\tau,t}(\hat{f})$ in two scenarios. The first one, considered in Theorem II.4, concerns the case when \mathcal{F} is a class of functions taking their values in $[-B, B]$ for some $B > 0$. A possible extension for unbounded classes is discussed in Theorem II.7.

Before we formulate the theoretical results rigorously, let us remind a reader some preliminaries on covering and bracketing numbers. Given a normed space $(\mathcal{F}, \|\cdot\|_{L_2(\mathfrak{p})})$ and $u > 0$, the covering number $\mathcal{N}(\mathcal{F}, L_2(\mathfrak{p}), u)$ is the minimal number of balls of radius u needed to cover \mathcal{F} . Further, for any $f_1, f_2 \in \mathcal{F}$, such that $f_1 \leq f_2$ almost surely, a bracket $[f_1, f_2]$ is a set of all such $g \in \mathcal{F}$ that $f_1 \leq g \leq f_2$ with probability one. The size of the bracket $[f_1, f_2]$ is $\|f_1 - f_2\|_{L_2(\mathfrak{p})}$. The bracketing number $\mathcal{N}_{[]}(\mathcal{F}, L_2(\mathfrak{p}), u)$ is the minimal number of brackets of size u needed to cover \mathcal{F} .

In the bounded case, we require the class \mathcal{F} to have a polynomial bracketing number. In Section III, we give an example that, if \mathfrak{p} is supported on a unit cube in \mathbb{R}^p , then a class of neural networks with ReLU activations satisfies this assumption.

Assumption II.3. *There exist positive constants A, B , and d , such that $\mathcal{D}(\mathcal{F}, L_\infty(\mathfrak{p})) \leq B$, and the bracketing number of the class \mathcal{F} with respect to the $L_2(\mathfrak{p})$ -norm satisfies the inequality*

$$\mathcal{N}_{[]}(\mathcal{F}, L_2(\mathfrak{p}), u) \leq \left(\frac{A}{u}\right)^d, \quad \text{for all } 0 < u \leq 2B.$$

We are in position to formulate a result about the large deviations of $\mathcal{T}_{\tau,t}(\hat{f}_{\tau,t})$.

Theorem II.4. *Grant Assumption II.3. Fix any $t \in \mathbb{N}$, any $\tau \in \{1, \dots, t-1\}$ and assume that X_1, \dots, X_t are i.i.d. random elements with the density \mathfrak{p} . Let $\hat{f} \in \operatorname{argmax}_{f \in \mathcal{F}} \mathcal{T}_{\tau,t}(f)$. Then, for any $\delta \in (0, 1)$, with probability at least $1 - \delta$, it holds that*

$$\mathcal{T}_{\tau,t}(\hat{f}) \lesssim de^B \left[B + \log \left(\frac{A\tau(t-\tau)}{td} \right) \right] + e^B \log(1/\delta). \quad (7)$$

Note that if $0 \in \mathcal{F}$ (which is a very mild requirement), then the statistic $\mathcal{T}_{\tau,t}(\hat{f})$ is non-negative. Theorem II.4 also shows that we use a proper scaling for $\mathcal{T}_{\tau,t}(\hat{f})$ in a sense that the high probability upper bound for $\mathcal{T}_{\tau,t}(\hat{f})$ has only a logarithmic dependence on τ .

Unfortunately, the boundedness of \mathcal{F} with respect to the $L_\infty(\mathfrak{p})$ -norm may be restrictive, especially if \mathfrak{p} has an unbounded support. In the rest of this section, we consider the case when $\mathcal{D}(\mathcal{F}, L_\infty(\mathfrak{p}))$ is allowed to be infinite.

Definition II.5. *A class of functions \mathcal{F} is called L -sub-Gaussian (with respect to a density \mathfrak{p}) if $\|f\|_{\psi_2(\mathfrak{p})} \leq L\|f\|_{L_2(\mathfrak{p})}$ for all $f \in \mathcal{F}$.*

A simple example of a sub-Gaussian class is the class of linear functions (with respect to a Gaussian measure). In Section III, we show that Algorithm II.1 with the linear class \mathcal{F} can efficiently detect a mean shift in a multivariate Gaussian sequence model. We also relax the bracketing number assumption and replace it by the next one.

Assumption II.6. *The class \mathcal{F} is L -sub-Gaussian for some constant $L > 0$. Besides, there exist positive constants A and d , such that the covering number of the class \mathcal{F} with respect to the $L_2(\mathfrak{p})$ -norm satisfies the inequality*

$$\mathcal{N}(\mathcal{F}, L_2(\mathfrak{p}), u) \leq \left(\frac{A}{u}\right)^d \quad \text{for all } 0 < u \leq \mathcal{D}(\mathcal{F}, L_2(\mathfrak{p})).$$

We are ready to formulate our main result concerning the behaviour of the statistic $\mathcal{T}_{\tau,t}(\hat{f}_{\tau,t})$ in the stationary regime in the unbounded case.

Theorem II.7. *Grant Assumption II.6. Fix any $t \in \mathbb{N}$, any $\tau \in \{1, \dots, t-1\}$ and assume that X_1, \dots, X_t are i.i.d. random elements with the density \mathfrak{p} . Let $\hat{f} \in \operatorname{argmax}_{f \in \mathcal{F}} \mathcal{T}_{\tau,t}(f)$. Then, for any $\delta \in (0, 1)$, with probability at least $1 - \delta$, it holds that*

$$\mathcal{T}_{\tau,t}(\hat{f}) \lesssim L^2 de^{\mathcal{D}(\mathcal{F}, \psi_2(\mathfrak{p}))\sqrt{2\log(4L\sqrt{2})}} \log(1/\delta) \cdot \left[\mathcal{D}(\mathcal{F}, \psi_2(\mathfrak{p}))\sqrt{\log L} + \log \left(\frac{A\tau(t-\tau)}{L^2td} \right) \right].$$

To sum up the results of Sections II-A and II-B, the test statistic S_t , defined in (5), is expected to grow steeply after the change point. On the other hand, it will be not too large in the stationary regime, when no change point occurs. Let us illustrate this point with a simple example. Let X_1, \dots, X_T , $T = 100$, be a sequence of i.i.d. observations drawn according to the Gaussian distribution $\mathcal{N}(0, 0.01)$. Let $\tau^* = 75$ and define a sequence Y_1, \dots, Y_T according to the formula

$$Y_t = \begin{cases} X_t, & \text{if } t \leq \tau^*, \\ 0.2 + X_t, & \text{otherwise.} \end{cases}$$

In other words, the sequences $\{X_t : 1 \leq t \leq T\}$ and $\{Y_t : 1 \leq t \leq T\}$ coincide before the change point τ^* and differ by the shift $\mu = 0.2$ after it. A realization of the sequences is displayed in Figure 1. Let $\mathcal{F} = \{f(x) = wx + b : w, b \in \mathbb{R}\}$ be a class of linear functions and apply Algorithm II.1 to the sequences described above. We observe that the test statistic S_t , computed for the sequence Y_1, \dots, Y_T (the solid red line in Figure 1), rises sharply after the change point (see Figure 1, bottom line) and achieves the value 17.5 in the end but, on the other hand, it does not exceed 2.5 in the stationary regime (see the dotted blue line in Figure 1).

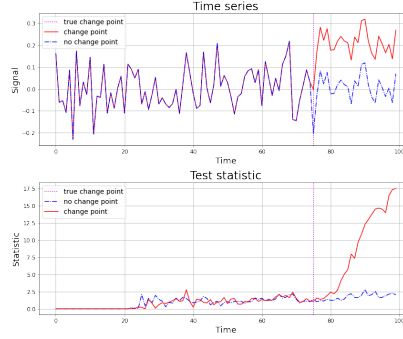


Figure 1. An example of behaviour of the test statistic S_t (defined in (5)) in the presence of a change point and in the stationary regime. Top line: a stationary sequence (blue) and a sequence of observations with a change point (red). Bottom line: corresponding values of the test statistic S_t with a linear class. The dashed vertical line corresponds to the true change point τ^* .

C. Bounds on the average running length and the expected detection delay

In this section, we provide lower bounds on the average running length and the expected detection delay of Algorithm II.1, based on our findings presented in Sections II-A and II-B. All the bounds hold with high probability.

Let us introduce $\rho(\mathcal{F}) = \inf_{f \in \mathcal{F}} \|\ln(p/q) - f\|_{L_2(p+q)}$. We have the following result for the case of \mathcal{F} with bounded diameter with respect to the $L_\infty(p)$ -norm.

Theorem II.8. *Grant Assumption II.3 and assume that $\|f\|_{L_\infty(q)} \leq B$ for all $f \in \mathcal{F}$. Fix any $\delta \in (0, 1)$ and $T \in \mathbb{N}$. There exists such a choice of \mathfrak{z} in Algorithm II.1 (specified in the proof) that the following holds:*

- if $\tau^* = \infty$, then Algorithm II.1 makes at least T steps until the false alarm with probability at least $1 - \delta$;
- otherwise, if τ^* is sufficiently large, so that it fulfils

$$\tau^* \geq \frac{B^2 \log(1/\delta)}{(\text{JS}(p, q) - \rho^2(\mathcal{F})/16)^2} + \frac{6B \log(1/\delta) + 2\mathfrak{z}}{(\text{JS}(p, q) - \rho^2(\mathcal{F})/16)},$$

then the stopping time \hat{t} of Algorithm II.1 satisfies the inequality

$$\hat{t} - \tau^* \lesssim \frac{B^2 \log(1/\delta)}{(\text{JS}(p, q) - \rho^2(\mathcal{F})/16)^2} + \frac{de^B [B + \log(AT/d)] + e^B \log(T/\delta)}{(\text{JS}(p, q) - \rho^2(\mathcal{F})/16)}$$

with probability at least $1 - \delta$.

Remark II.9. We emphasize that \hat{t} is the stopping time of the procedure, it should not be confused with an estimate of τ^* . A natural way to estimate the change point is to consider

$$\hat{\tau} = \operatorname{argmax}_{\tau \in \{1, \dots, \hat{t}\}} S_{\tau, \hat{t}}.$$

However, in the present paper, we focus on the running length and the detection delay only. We do not tackle the problem of estimation of τ^* . The study of theoretical properties of $\hat{\tau}$ is left for the future research.

Using a similar technique as in the proof of Theorem II.8 and Theorem II.7, we obtain large deviation bounds on the detection delay of Algorithm II.1 in the sub-Gaussian case.

Theorem II.10. *Grant Assumption II.6 and fix any $\delta \in (0, 1)$, $T \in \mathbb{N}$. There exists such a choice of \mathfrak{z} in Algorithm II.1 (specified in the proof) that the following holds:*

- if $\tau^* = \infty$, then Algorithm II.1 makes at least T steps until the false alarm with probability at least $1 - \delta$;
- otherwise, if τ^* is sufficiently large, then the stopping time \hat{t} of Algorithm II.1 satisfies the inequality

$$\begin{aligned} \hat{t} - \tau^* \lesssim & \frac{L^2 d \log(T/\delta) e^{\mathcal{D}(\mathcal{F}, \psi_2(p)) \sqrt{2 \log(4L\sqrt{2})}}}{(\text{JS}(p, q) - \rho^2(\mathcal{F})/16)} \cdot \left[\mathcal{D}(\mathcal{F}, \psi_2(p)) \sqrt{\log L} + \log \left(\frac{AT}{Ld} \right) \right] \\ & + \frac{[\mathcal{D}(\mathcal{F}, \psi_2(p)) \vee \mathcal{D}(\mathcal{F}, \psi_2(q))]^2 \log(1/\delta)}{(\text{JS}(p, q) - \rho^2(\mathcal{F})/16)^2} \end{aligned}$$

with probability at least $1 - \delta$.

Remark II.11. The results of Theorems II.8 and II.10 can be easily extended to the case of multiple change points. We just have to restart the procedure after a structural break was detected. The only additional requirement will be that the distance between two subsequent change points is $\Omega(\log T)$, which is quite standard for the offline setup.

We elaborate on the results of Theorems II.8 and II.10 in the next section.

III. EXAMPLES

In this section, we specify the results of Theorem II.8 and Theorem II.10 for particular cases. Our examples include nonparametric change point detection via feed-forward neural networks and the classical problem of mean shift detection in a Gaussian sequence model.

A. Nonparametric online change point detection via neural networks

Consider the following nonparametric change point detection setup. Let X_1, \dots, X_t, \dots be independent random elements and assume that X_1, \dots, X_{τ^*} have a density \mathbf{p} supported on $[0, 1]^p$ while the other elements of the time series are drawn from the density \mathbf{q} (also supported on the unit cube $[0, 1]^p$). Assume that $\ln(\mathbf{p}/\mathbf{q})$ belongs to a Hölder class $\mathcal{H}^\beta([0, 1]^p, H)$ for some smoothness parameter $\beta > 0$ and some $H > 0$. Recall that the class $\mathcal{H}^\beta([0, 1]^p, H)$ is defined as

$$\mathcal{H}^\beta([0, 1]^p, H) = \left\{ f : [0, 1]^p \rightarrow \mathbb{R} : \sum_{\substack{\alpha \in \mathbb{Z}_+^p: \\ \|\alpha\|_1 < \beta}} \|\partial^\alpha f\|_{L_\infty([0, 1]^p)} + \sum_{\substack{\alpha \in \mathbb{Z}_+^p: \\ \|\alpha\|_1 = \lfloor \beta \rfloor}} \sup_{\substack{x, y \in [0, 1]^p \\ x \neq y}} \frac{|\partial^\alpha f(x) - \partial^\alpha f(y)|}{\|x - y\|_\infty^{\beta - \lfloor \beta \rfloor}} \leq H \right\},$$

where, for any multi-index $\alpha = (\alpha_1, \dots, \alpha_p)$, $\partial^\alpha f(x)$ stands for the partial derivative $\partial^{\alpha_1} \dots \partial^{\alpha_p} f(x) / (\partial x_1^{\alpha_1} \dots \partial x_p^{\alpha_p})$ and, for any $\beta \in \mathbb{R}$, $\lfloor \beta \rfloor$ denotes the largest integer strictly less than β . We use a class of feed-forward neural networks to detect a change in the distribution of the observed sequence. Introduce the ReLU activation function $\sigma(u) = (u \vee 0)$, $u \in \mathbb{R}$, and, for any $v \in \mathbb{R}^p$, define the *shifted* activation function σ_v as $\sigma_v(x) = (\sigma(x_1 - v_1), \dots, \sigma(x_p - v_p))^\top$, $x \in \mathbb{R}^p$. A neural network is a composition of linear and nonlinear maps. Let us fix a number of hidden layers $L \in \mathbb{N}$, an architecture $\mathcal{A} = (a_0, \dots, a_{L+1}) \in \mathbb{N}^{L+2}$, matrices $W_1 \in \mathbb{R}^{a_1 \times a_0}, \dots, W_{L+1} \in \mathbb{R}^{a_{L+1} \times a_L}$, and shift vectors $v_1 \in \mathbb{R}^{a_1}, \dots, v_L \in \mathbb{R}^{a_L}$. Then a neural network with ReLU activations, L hidden layers and the architecture \mathcal{A} is a function $f : \mathbb{R}^{a_0} \rightarrow \mathbb{R}^{a_{L+1}}$ of the form

$$f = W_L \circ \sigma_{v_L} \circ W_{L-1} \circ \sigma_{v_{L-1}} \circ \dots \circ W_1 \circ \sigma_{v_1} \circ W_0. \quad (8)$$

Given $L \in \mathbb{N}$, $\mathcal{A} = (p, a_1, \dots, a_L, 1) \in \mathbb{N}^{L+2}$, and $s \in \mathbb{N}$, we consider a class of sparsely connected neural networks

$$\text{NN}(L, \mathcal{A}, s) = \left\{ f \text{ of the form (8)} : \max_{i,j} |W_{ij}| \vee \max_i |v_i| \leq 1, \|W_0\|_0 + \sum_{j=1}^L (\|W_j\|_0 + \|v_j\|_0) \leq s \right\}.$$

To our knowledge, this class of neural networks was first studied in [50]. The sparsity parameter s is introduced to reflect the fact that, in practice, one rarely uses fully connected neural networks, and the number of active neurons is usually much smaller than the total number of parameters $\sum_{j=1}^L a_j + \sum_{j=1}^{L+1} a_{j-1} a_j$. In [50], the author proves two important results, concerning approximation properties (Theorem 5) and the covering number of the class $\text{NN}(L, \mathcal{A}, s)$ (Lemma 5). We provide their statements in Appendix B to make the paper self-contained. Combining these results with Theorem II.8, we get the following corollary.

Corollary III.1. *Assume that $\ln(\mathbf{p}/\mathbf{q}) \in \mathcal{H}^\beta([0, 1]^p, H)$. Fix any $\delta \in (0, 1)$ and $T \in \mathbb{N}$. There exist $C > 0$, $\tau_0 \in \mathbb{N}$, $L \in \mathbb{Z}_+$, $\mathcal{A} \in \mathbb{N}^{L+2}$, $s \in \mathbb{N}$, and $\mathfrak{z} > 0$ (specified in the proof) such that the following holds. Run Algorithm II.1 with the class of truncated neural networks*

$$\text{NN}_B(L, \mathcal{A}, s) = \{g(x) = -B \vee (f(x) \wedge B) : f \in \text{NN}(L, \mathcal{A}, s)\},$$

where B any number greater than $H + \sqrt{\text{JS}(\mathbf{p}, \mathbf{q})}$. If $\tau^* = \infty$, then Algorithm II.1 stops after at least T steps with probability at least $1 - \delta$. Otherwise, if τ^* is sufficiently large, then, with probability at least $1 - \delta$, the stopping time \hat{t} of Algorithm II.1 fulfils

$$\hat{t} - \tau^* \lesssim \frac{e^B \log(1/\text{JS}(\mathbf{p}, \mathbf{q})) [B + \log(1/\text{JS}(\mathbf{p}, \mathbf{q})) \log T]}{\text{JS}(\mathbf{p}, \mathbf{q})^{\frac{2\beta+2}{2\beta}}} + e^B \log(T/\delta) + \frac{B^2 \log(1/\delta)}{\text{JS}(\mathbf{p}, \mathbf{q})^2},$$

where the hidden constant depends on H, β , and p .

To our knowledge, this is the first non-asymptotic high probability bound on the detection delay for an online change point detection procedure exploiting neural networks.

B. Online detection of a mean shift in a Gaussian sequence model

In this section, we show how the result of Theorem II.10 applies to the classical problem of mean shift detection in a Gaussian sequence. Assume that X_1, \dots, X_{τ^*} are i.i.d. random vectors in \mathbb{R}^p with the Gaussian distribution $\mathcal{N}(0, \Sigma)$ while

$X_{\tau^*+1}, \dots, X_t, \dots$ have the Gaussian distribution $\mathcal{N}(\mu, \Sigma)$, $\mu \neq 0$. In this case, $\ln(p/q)$ is linear, so it is reasonable to consider the following class of functions:

$$\mathcal{F}_{\text{lin}} = \{f_{w,b}(x) = w^\top x + b : \|\Sigma^{1/2}w\| \leq \|\Sigma^{-1/2}\mu\|, |b| \leq \mu^\top \Sigma^{-1}\mu\}. \quad (9)$$

With this choice, $f^* \in \mathcal{F}_{\text{lin}}$, that is, the approximation error is equal to zero. At the same time, the class \mathcal{F}_{lin} is sub-Gaussian, its ψ_2 -diameter is of order $(\mu^\top \Sigma^{-1}\mu)^{1/2}$, and its metric entropy satisfies the inequality $\log \mathcal{N}(\mathcal{F}_{\text{lin}}, L_2(p), \varepsilon) \lesssim p \log(\mu^\top \Sigma^{-1}\mu/\varepsilon)$ for any $\varepsilon > 0$. Substituting these bounds into the statement of Theorem II.10, we get the following corollary.

Corollary III.2. *Assume that $\|\Sigma^{-1/2}\mu\| \leq \ln(4/3)$. Fix any $\delta \in (0, 1)$ and $T \in \mathbb{N}$. There exists such $\mathfrak{z} > 0$ that the following holds:*

- if $\tau^* = \infty$, then the running length of Algorithm II.1 (with the class \mathcal{F}_{lin} given by (9)) is at least T on an event with probability $1 - \delta$;
- otherwise, if τ^* is sufficiently large, then the stopping time \hat{t} of Algorithm II.1 (with the class \mathcal{F}_{lin}) satisfies the inequality

$$\hat{t} - \tau^* \lesssim \frac{p \log(\|\Sigma^{-1/2}\mu\|T/p) \log(T/\delta)}{\mu^\top \Sigma^{-1}\mu}$$

with probability at least $1 - \delta$.

The number $\|\Sigma^{-1/2}\mu\|$ is sometimes referred to as signal-to-noise ratio (SNR) in the change point detection literature. For the ease of presentation, we consider only the case of low SNR. Corollary III.2 shows that our approach captures the dependence on $\|\Sigma^{-1/2}\mu\|$ correctly (cf. [64, Theorem 1] and [7, Theorem 2]). However, it has an additional logarithmic term compared to the worst-case detection delay of the CUSUM-type procedure [64]. This artefact appears because of universality of our algorithm: it tries to learn an optimal discriminator D without any prior knowledge about p and q nor about the kind of change, while the CUSUM-type procedure [64] exploits the difference in means of the pre-change and post-change distributions.

IV. A FASTER VERSION OF THE ALGORITHM

In Section II, we discussed that Algorithm II.1 requires $O(t^2 \log(1/\varepsilon) \wedge t/\varepsilon)$ operations on each round to compute \mathcal{S}_t within the accuracy ε . It is a reasonable runtime but the procedure requires to solve several optimization problems on each round. The goal of this section is to suggest a faster version of Algorithm II.1. Our main idea is to update the estimates $\hat{\theta}_{\tau,t}$ in a recursive manner, using the results from the previous iterations. This leads to significant acceleration of the procedure.

Our approach relies on the tools from online convex optimization, so let us recall its framework to the reader before we move to the description of the algorithm. We also refer to the brilliant surveys of Shalev-Shwartz [51] and Hazan [25] for the introduction and basic algorithms on this topic. Online convex optimization is a repeating game between a learner (also referred to as player) and his opponent (or adversary). On the round t , the player chooses a prediction \hat{p}_t from a given convex compact set \mathfrak{P} . After that, the opponent reveals a convex function $\ell_t : \mathfrak{P} \rightarrow \mathbb{R}$, and the learner suffers the loss $\ell_t(\hat{p}_t)$. The player's performance is measured by the regret after T rounds, defined as

$$R_T = \sum_{t=1}^T \ell_t(\hat{p}_t) - \min_{p \in \mathfrak{P}} \left(\sum_{t=1}^T \ell_t(p) \right).$$

The goal of the player is to make R_T as small as possible regardless the opponent's strategy. We summarize the described framework below.

Online convex optimization framework.

- A convex compact set \mathfrak{P} is given.
- **For** $t = 1, 2, \dots, T, \dots$:
 - 1) the learner makes a prediction \hat{p}_t ;
 - 2) the adversary reveals a convex function ℓ_t ;
 - 3) the learner suffers the loss $\ell_t(\hat{p}_t)$.

In the context of sequential change point detection, the online convex optimization framework was applied in the paper of Cao, Xie, Xie, and Xu [5]. However, the authors imposed strong parametric assumptions on the density of observations. In particular, the pre-change and post-change densities, p and q respectively, must belong to an exponential family with known link function. In our approach, we escape such problems, because we make an assumption about the class \mathcal{F} , which we are free to choose. From now on, we assume that \mathcal{F} is a parametric class of the form

$$\mathcal{F} = \{f_\theta(x) = \theta^\top \psi(x) : \theta \in \Theta\}, \quad (10)$$

where Θ is a compact convex subset of a Euclidean space and ψ is a fixed vector-function. Since any function from \mathcal{F} is completely defined by the value of θ , we adopt the notation

$$\mathcal{T}_{\tau,t}(\theta) \equiv \mathcal{T}_{\tau,t}(f_\theta), \quad \theta \in \Theta,$$

where $\mathcal{T}_{\tau,t}$ is defined in (4). The parametrization (10) prevents \mathcal{F} from being, for instance, a class of neural networks. On the other hand, we must ensure that \mathcal{F} is convex in order to apply the tools from online convex optimization. Moreover, the representation (10) still includes several important and useful examples, which show a reasonable performance in numerical experiments. We provide more details a bit later, in Section V.

We are ready to describe the idea of the method. Note that, for any $t \in \mathbb{N}$, any $\tau \in \{1, \dots, t-1\}$, and any $\theta \in \Theta$, the statistic $\mathcal{T}_{\tau,t}(\theta)$ satisfies the equality

$$\begin{aligned} t\mathcal{T}_{\tau,t}(\theta) - (t-1)\mathcal{T}_{\tau,t-1}(\theta) &= -(t-\tau) \sum_{s=1}^{\tau} \ln \left(\frac{1 + e^{-\theta^\top \psi(X_s)}}{2} \right) - \tau \sum_{s=\tau+1}^t \ln \left(\frac{1 + e^{\theta^\top \psi(X_s)}}{2} \right) \\ &\quad + (t-1-\tau) \sum_{s=1}^{\tau} \ln \left(\frac{1 + e^{-\theta^\top \psi(X_s)}}{2} \right) + \tau \sum_{s=\tau+1}^{t-1} \ln \left(\frac{1 + e^{\theta^\top \psi(X_s)}}{2} \right) \\ &= - \sum_{s=1}^{\tau} \ln \left(\frac{1 + e^{-\theta^\top \psi(X_s)}}{2} \right) - \tau \ln \left(\frac{1 + e^{\theta^\top \psi(X_t)}}{2} \right). \end{aligned}$$

With the convention

$$\mathcal{T}_{\tau,t}(\theta) = 0 \quad \text{for any } \tau \geq t \text{ and } \theta \in \Theta,$$

we can express $t\mathcal{T}_{\tau,t}(\theta)$ recursively in the following form:

$$-t\mathcal{T}_{\tau,t}(\theta) = -(t-1)\mathcal{T}_{\tau,t-1}(\theta) + \varphi_{\tau,t}(\theta),$$

where

$$\varphi_{\tau,t}(\theta) = \begin{cases} \sum_{s=1}^{\tau} \ln \left(1 + e^{-\theta^\top \psi(X_s)} \right) + \tau \ln \left(1 + e^{\theta^\top \psi(X_t)} \right) - 2\tau \ln 2, & \text{if } \tau \leq t-1, \\ 0, & \text{otherwise.} \end{cases} \quad (11)$$

Let us fix any $\tau \in \mathbb{N}$ and run the online convex optimization game with the domain $\mathfrak{P} = \Theta$ and the loss $\ell_t(\theta) = \varphi_{\tau,t}(\theta)$ (which is convex). Assume that the player made predictions $\hat{\theta}_{\tau,1}, \dots, \hat{\theta}_{\tau,t}$ on the first t rounds. If his strategy is good enough, then the cumulative loss after t rounds

$$\sum_{s=1}^t \varphi_{\tau,s}(\hat{\theta}_{\tau,s})$$

will be close to

$$\min_{\theta \in \Theta} \left(\sum_{s=1}^t \varphi_{\tau,s}(\theta) \right) = -t \max_{\theta \in \Theta} \mathcal{T}_{\tau,t}(\theta).$$

Hence, for any $\tau \in \{1, \dots, t-1\}$, we can estimate $\max_{\theta \in \Theta} \mathcal{T}_{\tau,t}(\theta)$ by

$$\hat{\mathcal{T}}_{\tau,t} = -\frac{1}{t} \sum_{s=1}^t \varphi_{\tau,s}(\hat{\theta}_{\tau,s}) = \frac{t-1}{t} \hat{\mathcal{T}}_{\tau,t-1} - \frac{1}{t} \varphi_{\tau,t}(\hat{\theta}_{\tau,t})$$

and then use the statistic $\hat{\mathcal{S}}_t = \max_{1 \leq \tau \leq t-1} \hat{\mathcal{T}}_{\tau,t}$, instead of \mathcal{S}_t , defined in (5).

The only question remains is how to compute the predictions $\hat{\theta}_{\tau,1}, \dots, \hat{\theta}_{\tau,t}$, because there are plenty of online convex optimization algorithms, and we have to choose one, which is more suitable for our setup. Note that the function $G(u) = \ln(1 + e^u)$ is Lipschitz and strongly convex on any compact set (of course, the strong convexity constant depends on the set). Hence, for any $\tau \in \{1, \dots, t-1\}$, the loss $\varphi_{\tau,t}(\theta)$ is a superposition of strongly convex and linear functions. The losses of such form were considered in the paper of Hazan, Agarwal, and Kale [26]. The authors showed that the follow the approximate leader (FTAL) algorithm achieves logarithmic regret in this situation. We find FTAL to be an appropriate choice for our purposes. We also note that the loss function $\varphi_{\tau,t}(\theta)$ is exp-concave on the convex compact set Θ , and thus, one can use, for instance, online Newton step (ONS), which also has the $O(\log T)$ regret guarantees, instead of FTAL. The reason that we use FTAL, rather than ONS, is that the former algorithm has less hyperparameters, which simplifies the tuning procedure. We provide the pseudocode of the described procedure in Algorithm IV.1

Algorithm IV.1 (FALCON, fast algorithm based on contrastive approach).

- **Input:** a class of functions \mathcal{F} of the form (10), a parameter $\beta > 0$, and a threshold $\mathfrak{z} > 0$.
- **Initialization:** $\hat{\theta}_{\tau,t} = 0$ and $\hat{\mathcal{T}}_{\tau,t} = 0$ for all $\tau \geq t$.
- **For** $t = 1, 2, \dots$ **do** the following.

- 1) Receive an observation X_t .
- 2) For each $\tau \in \{1, \dots, t-1\}$, compute the gradients

$$g_{\tau,t} = \nabla \varphi_{\tau,t}(\hat{\theta}_{\tau,t-1}) = \begin{cases} \left(-\sum_{s=1}^{\tau} \frac{e^{-\theta^\top \psi(X_s)}}{1+e^{-\theta^\top \psi(X_s)}} \psi(X_s) + \frac{\tau e^{\theta^\top \psi(X_t)}}{1+e^{\theta^\top \psi(X_t)}} \psi(X_t) \right) \Big|_{\theta=\hat{\theta}_{\tau,t-1}}, & \text{if } \tau \leq t-1, \\ 0, & \text{otherwise,} \end{cases}$$

calculate

$$A_{\tau,t} = \sum_{s=1}^t g_{\tau,s} g_{\tau,s}^\top = A_{\tau,t-1} + g_{\tau,t} g_{\tau,t}^\top$$

and

$$b_{\tau,t} = \sum_{s=1}^t \left(g_{\tau,s} g_{\tau,s}^\top \hat{\theta}_{\tau,s-1} - \frac{1}{\beta} g_{\tau,s} \right) = b_{\tau,t-1} + g_{\tau,t} g_{\tau,t}^\top \hat{\theta}_{\tau,t-1} - \frac{1}{\beta} g_{\tau,t}.$$

- 3) For each $\tau \in \{1, \dots, t-1\}$, update the estimates $\hat{\theta}_{\tau,t}$ according to the formula

$$\hat{\theta}_{\tau,t} \in \underset{\theta \in \Theta}{\operatorname{argmin}} (\theta - A_t^\dagger b_t)^\top A_t (\theta - A_t^\dagger b_t), \quad (12)$$

where A_t^\dagger stands for the Moore-Penrose pseudoinverse of the matrix A_t .

- 4) For each $\tau \in \{1, \dots, t-1\}$, compute

$$\hat{\mathcal{T}}_{\tau,t} = -\frac{1}{t} \sum_{s=1}^t \varphi_{\tau,s}(\hat{\theta}_{\tau,s-1}) = \frac{t-1}{t} \hat{\mathcal{T}}_{\tau,t-1} - \frac{1}{t} \varphi_{\tau,t}(\hat{\theta}_{\tau,t-1}),$$

where the function $\varphi_{\tau,t}(\theta)$ is defined in (11).

- 5) Compute the test statistic

$$\hat{\mathcal{S}}_t = \max_{1 \leq \tau \leq t-1} \hat{\mathcal{T}}_{\tau,t},$$

- 6) If $\hat{\mathcal{S}}_t > \mathfrak{z}$, terminate the procedure, and report the change point occurrence.

- **Return.**

The update of $\hat{\theta}_{\tau,t}$ is implicit, so let us discuss its computational complexity. Of course, the solution of the optimization subroutine (12) heavily depends on the domain Θ . In the numerical experiments, we take Θ as a ball in Euclidean space, so the problem (12) can be solved directly in $O(1)$ operations by the means of matrix factorizations. Algorithm IV.1 saves a lot of time, because $A_{\tau,t}$, $b_{\tau,t}$, and $\hat{\mathcal{T}}_{\tau,t}$ are computed recursively using the values from the previous iteration.

V. NUMERICAL EXPERIMENTS

In this section, we illustrate the performance of our procedure on synthetic and real-world data sets. The code for all the experiments, described below, is available at Github¹. We consider two variants of the class \mathcal{F} used in Algorithm II.1: polynomials of degree p and the class of fully connected feed-forward neural networks with architecture (1, 2, 3, 1) and ReLU activations. The neural network architecture was the same in all the experiments. We truncate the function values if their absolute value exceeds 10 to avoid numerical issues. Though the class \mathcal{F} II.1 can be arbitrary in general, Theorems II.8 and II.10 imply that it should be expressive enough to approximate the log-ratio $\ln(p/q)$ with an adequate accuracy. Our choice is motivated by the fact that polynomials and feed-forward neural networks with ReLU activations are known to have the universal approximation property. Concerning Algorithm IV.1, we have an additional requirement for the class \mathcal{F} to be convex. For this reason, we cannot take \mathcal{F} the same as in Algorithm II.1 (we would like to note that the class of truncated polynomials is non-convex). Instead, we used linear combinations of Hermite or Legendre polynomials of degree p with vectors of coefficients lying in the Euclidean ball $\mathcal{B}(0, 10)$.

The performance of our method (with three aforementioned variants of the class \mathcal{F}) is compared with two popular non-parametric change point detection methods: KLIEP [55, 38] and kernel change point detection with M-statistic [36]. We also added the comparison with CUSUM (see, e.g., [61, Definition 1]) in the experiment with a shift in expectation. KLIEP is a

¹https://github.com/npuchkin/contrastive_change_point_detection_extended

density-ratio-based change point detection method, estimating of the KL-divergence between the pre-change and post-change distributions. As we discussed in Section II-A, our approach is somehow related to density-ratio-based methods, so it is reasonable to compare our algorithm with one of them. In [36], the authors use kernel methods to approximate the squared maximum mean discrepancy (MMD) between the pre-change and post change distributions. We use a different divergence measure, based on the maximum cross-entropy, but the core idea of maximizing discrepancy between pre-change and post change observations is quite similar. Both KLIEP and M-statistic require a bandwidth parameter b for their computation. In our experiments, we tune this parameter in a way to minimize the detection delay, provided that the number of false alarms or the running length is acceptable.

A. Synthetic data sets

The experiments with synthetic data check the ability of the procedure to detect changes in mean, variance, and the density of the distribution. We considered the following setups.

Example 1: mean shift detection in a Gaussian sequence model. We generated a univariate Gaussian sequence of length 150. The first 75 observations had the Gaussian distribution $\mathcal{N}(0, \sigma^2)$ with $\sigma = 0.1$ and the other 75 were i.i.d. $\mathcal{N}(\mu, \sigma^2)$ with $\mu = 0.2$ and the same σ .

Example 2: variance change detection in a Gaussian sequence model. In the second example, we sampled 75 independent Gaussian random variables $\mathcal{N}(0, \sigma_0^2)$ with $\sigma_0 = 0.1$ and 75 random variables with the distribution $\mathcal{N}(0, \sigma^2)$, $\sigma = 0.3$, so the expectation of all the random variables was the same. CUSUM is not applicable in this case, because it is designed to detect a mean shift.

Example 3: distributional change. Finally, we checked the ability of our procedure to adapt to distributional changes. For this purpose, we generated a sequence of 200 independent random variables where the first 75 had the uniform distribution on $[-\sigma/\sqrt{3}, \sigma/\sqrt{3}]$ with $\sigma = 0.1$ and the other 125 were drawn from the Gaussian distribution $\mathcal{N}(0, \sigma^2)$. The parameters of the uniform distribution were chosen in a way to match the first two moments of the Gaussian distribution. In this case, CUSUM is not applicable.

Table I

THE THRESHOLDS \mathfrak{z} AND THE VALUES OF HYPERPARAMETERS OF THE COMPETING ALGORITHMS IN THE EXPERIMENTS ON SYNTHETIC DATA SETS.

METHOD	EXAMPLE 1		EXAMPLE 2		EXAMPLE 3	
	\mathfrak{z}	PARAMETER	\mathfrak{z}	PARAMETER	\mathfrak{z}	PARAMETER
Algorithm II.1 + polynomials	2.46	$p = 1$	3.98	$p = 2$	3.51	$p = 5$
Algorithm II.1 + neural networks	4.38	-	4.38	-	2.77	-
Algorithm IV.1	1.81	$p = 1, \beta = 0.01$	2.27	$p = 2, \beta = 0.01$	1.2247	$p = 5, \beta = 0.005$
KLIEP	6.03	$b = 0.2$	4.16	$b = 0.33$	0.17	$b = 0.5$
M-statistic	9.59	$b = 0.5$	36.75	$b = 0.1$	0.26	$b = 0.5$
CUSUM	0.45	-	-	-	-	-

Before we move to the description of our results, let us first elaborate on the threshold tuning procedure. We sample $T = 150$ i.i.d. samples according to p and compute the maximal value of the corresponding test statistic $\mathcal{S}_t^{(1)}$, $1 \leq t \leq 150$. We repeat the procedure several times and obtain the values $\max_{1 \leq y \leq T} \mathcal{S}_t^{(2)}, \dots, \max_{1 \leq y \leq T} \mathcal{S}_t^{(J)}$, where J is the number of repetitions. Then we put

$$\mathfrak{z} = \max_{1 \leq j \leq J} \max_{1 \leq t \leq T} \mathcal{S}_t^{(j)}.$$

Such a choice ensures that the running length of our procedure is not smaller than $T = 150$ with probability at least $1 - 1/(J+1)$. Indeed, if we run the procedure in the stationary regime and compute the corresponding values of the test statistic \mathcal{S}_t , then the probability that $\max_{1 \leq t \leq T} \mathcal{S}_t$ exceeds $\mathfrak{z} = \max_{1 \leq j \leq J} \max_{1 \leq t \leq T} \mathcal{S}_t^{(j)}$ is the same as $\max_{1 \leq t \leq T} \mathcal{S}_t^{(j)}$ exceeds

$$\max \left\{ \max_{1 \leq t \leq T} \mathcal{S}_t, \max_{k \neq j} \max_{1 \leq t \leq T} \mathcal{S}_t^{(k)} \right\}.$$

Since all such probabilities sum to one, we conclude that $\mathbb{P}(\max_{1 \leq t \leq T} \mathcal{S}_t > \mathfrak{z}) = 1/(J+1)$, provided that there are no change points. We took $J = 9$ in the experiments with changes in mean and in variance. In the third experiment, where distribution of observations transforms but the first two moments remain unchanged, we took a smaller threshold equal to the average of $\max_{1 \leq t \leq T} \mathcal{S}_t^{(j)}$, $1 \leq j \leq J = 4$. However, this did not lead to false alarms. The thresholds of other algorithms were tuned in a similar fashion. The information about thresholds in the experiments with artificial data is collected in Table I.

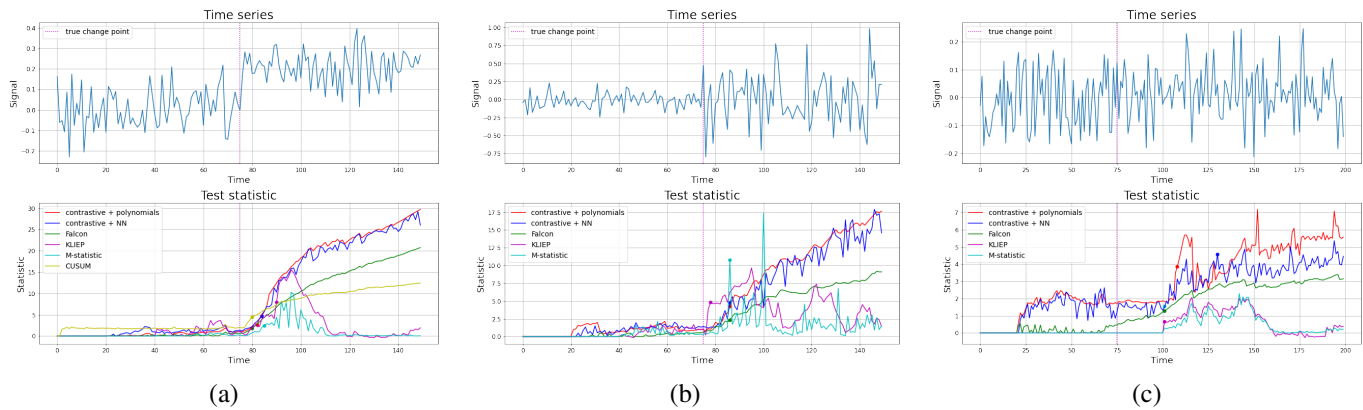


Figure 2. Examples of change point detection on synthetic data sets. Top line: the sequence of observations. Bottom line: corresponding values of test statistics S_t for Algorithm II.1 with two variants of the base class \mathcal{F} (polynomials (red) and neural networks (blue)), FALCON (Algorithm IV.1, green), CUSUM for mean shift detection (yellow), KLIEP (magenta) and M-statistics (cyan). The dashed vertical line corresponds to the true change point τ^* . The circle markers on solid lines correspond to the detection moments. Column (a): mean shift detection in a Gaussian sequence model (Example 1). Column (b): variance change detection in a Gaussian sequence model (Example 2). Column (c): distributional change (Example 3).

The setup was as follows. In each example, we sampled an artificial sequence 10 times and computed the average detection delays for Algorithm IV.1 with Hermite polynomials of degree $p = 1$, Algorithm II.1 with truncated polynomials of degree $p = 1$ different classes \mathcal{F} and for the competitors (CUSUM, KLIEP and kernel change point detection with M-statistic) for each realization. The results are displayed in Table II and Figure 2. In all the synthetic experiments, the weights of the neural network were optimized via the PyTorch implementation of the Adam method [31] with 50 epochs and the learning rate 0.1. During the first 20 iterations, we collected the observations for further training, and the test statistic was not computed. We also slightly adjusted the test statistic S_t : instead of maximizing $\mathcal{T}_{\tau,t}(\hat{f}_{\tau,t})$ over the whole set $\{1, \dots, t-1\}$, we took the maximum with respect to $\tau \in \{10, 11, \dots, t-10\}$. This simple trick helped us to reduce the detection delay. The hyperparameters of KLIEP and M-statistic-based kernel change point methods were tuned in a way to minimize the average detection delay while keeping the running length at least 150 with high probability.

Table II
DETECTION DELAYS OF ALGORITHM II.1 WITH TWO VARIANTS OF THE CLASS \mathcal{F} (POLYNOMIALS AND NEURAL NETWORKS), FALCON (ALGORITHM IV.1), KLIEP, KERNEL CHANGE POINT WITH M-STATISTIC, AND CUSUM ON SYNTHETIC DATA SETS. TWO BEST RESULTS ARE BOLDFACED.

METHOD	EXAMPLE 1	EXAMPLE 2	EXAMPLE 3
Algorithm II.1 + polynomials	6.7 ± 2.0	16.4 ± 8.1	58.4 ± 34.8
Algorithm II.1 + neural networks	8.9 ± 1.2	18.7 ± 9.2	38.0 ± 14.1
Algorithm IV.1	5.5 ± 1.7	14.1 ± 5.9	17.6 ± 14.7
KLIEP	8.9 ± 3.6	19.2 ± 18.4	26.8 ± 1.6
M-statistic	10.4 ± 3.4	51.1 ± 27.3	27.8 ± 2.2
CUSUM	5.0 ± 2.0	—	—

According to Table II, Algorithm IV.1 is the most efficient method to detect a change point amongst competitors. It only loses CUSUM in the mean shift detection example. That is not surprising, because CUSUM was especially designed to detect changes in mean of a Gaussian sequence. Algorithm II.1 with \mathcal{F} equal to the class of polynomials is quite close to Algorithm IV.1 in the first two experiments, but loses KLIEP and M-statistic based detector in the third example. However, in the first two examples all three our algorithms outperform both nonparametric baselines. We move to the experiments on the real-world data sets.

B. Univariate data I: speech records analysis

We used CENSREC-1-C² data in the Speech Resource Consortium (SRC) corpora provided by National Institute of Informatics (NII) to test the algorithm in practical tasks. The data set contains a clean speech record (MAH_clean) and the same record corrupted with noise of different magnitude (MAH_N1_SNR20, MAH_N1_SNR15). The signal plots are showed in Figure 3. We preprocessed the data as follows. First, we normalized the data. Next, we chose 10 segments with a single change from silence/noise to speech, and then each 10-th observation was taken. The first four segments were used to tune the hyperparameters and the thresholds and the other six were for testing. The true change point values were set on the MAH_clean data set and used in the noisy versions of the record. Examples of behaviour of test statistics for different methods are exposed in Figure 4.

²<http://research.nii.ac.jp/src/en/CENSREC-1-C.html>

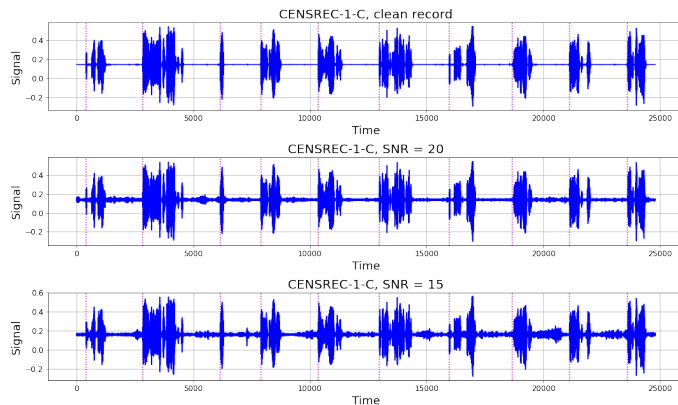


Figure 3. The CENSREC-1-C speech records with different amount of noise.

As in the experiments with the artificial data sets, we considered Algorithm II.1 with two variants of the class \mathcal{F} : polynomials of degree $p = 2$ and the class of fully connected feed-forward neural networks with architecture $(1, 2, 3, 1)$ and ReLU activations. We used the Adam optimizer with 20 epochs and the learning rate 0.1 to tune the parameters of the neural network. In Algorithm IV.1, the class \mathcal{F} was equal to linear combinations of Hermite polynomials of degree less than 3. The bandwidths used in KLIEP and the M-statistic based algorithm are shown in Table III. It also contains the corresponding values of thresholds. We computed detection delays for each algorithm on each of 6 test segments. The results are reported in Table IV.

Table III

THE THRESHOLDS \mathfrak{z} AND THE VALUES OF HYPERPARAMETERS OF THE COMPETING ALGORITHMS IN THE EXPERIMENTS ON THE CENSREC-1-C DATA SET.

	CLEAN RECORD		SNR20		SNR15	
	\mathfrak{z}	PARAMETER	\mathfrak{z}	PARAMETER	\mathfrak{z}	PARAMETER
Algorithm II.1 + polynomials	2.50	$p = 2$	10.24	$p = 2$	0.41	$p = 2$
Algorithm II.1 + neural networks	$3.39 \cdot 10^{-4}$	-	$2.27 \cdot 10^{-3}$	-	$4 \cdot 10^{-3}$	-
Algorithm IV.1	0.01	$p = 2, \beta = 0.5$	0.19	$p = 2, \beta = 0.02$	0.18	$p = 2, \beta = 0.01$
KLIEP	0.61	$b = 0.2$	1.17	$b = 0.075$	0.079	$b = 0.1$
M-statistic	$4.68 \cdot 10^{-3}$	$b = 0.1$	$15.7 \cdot 10^{-3}$	$b = 0.5$	10^{-4}	$b = 2$

Similarly to the experiments with artificial data, we have an algorithm, which outperforms others in all three situations. Namely, this is Algorithm II.1 with the class of neural networks. Algorithm IV.1 shows better performance than the kernel change point detection method in the case of clean record and when SNR is equal to 15 and it slightly loses in the case SNR = 15. In contrast to the experiments on synthetic data sets, KLIEP behaves poorly in this example.

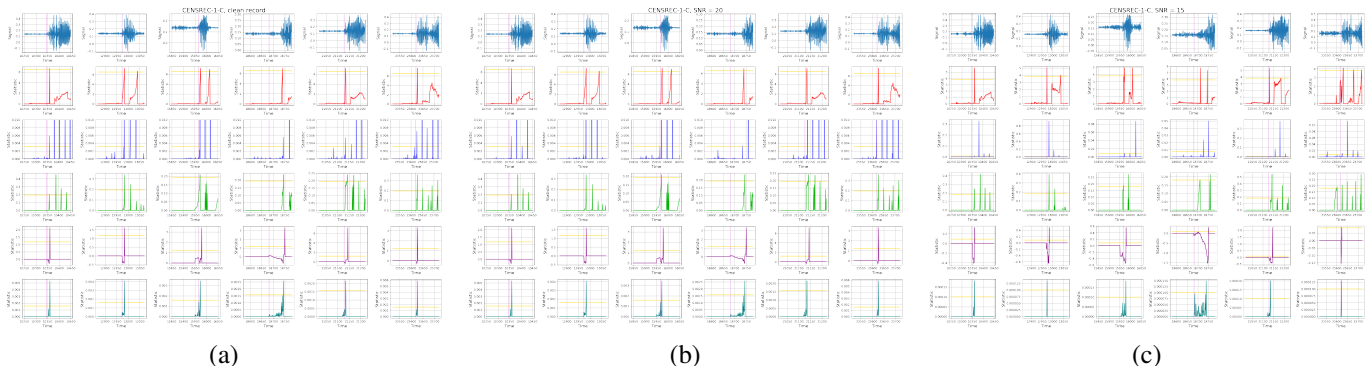


Figure 4. Examples of change point detection on the CENSREC-1-C data set (test part). The top line displays the sequence of observations. The other rows show the corresponding values of the test statistics for Algorithm II.1 with polynomials of degree $p = 2$ (red), Algorithm II.1 with neural networks (blue), Algorithm IV.1 with polynomials of degree $p = 2$ (green), KLIEP (magenta), and M-statistics (cyan). The dashed vertical and the yellow horizontal line correspond to the true change point τ^* and the threshold \mathfrak{z} , respectively. Column (a): clean speech record. Column (b): speech record corrupted with noise, SNR = 20. Column (c): speech record corrupted with noise, SNR = 15.

Table IV
AVERAGE DETECTION DELAYS (DD) AND THE NUMBER OF FALSE ALARMS (FA) OF ALGORITHM II.1 (WITH TWO VARIANTS OF THE CLASS \mathcal{F}), ALGORITHM IV.1, KLIEP, AND KERNEL CHANGE POINT DETECTOR WITH M-STATISTIC ON THE CENSREC-1-C SPEECH RECORDS WITH DIFFERENT NOISE LEVEL. TWO BEST RESULTS ARE BOLDFACED.

	CLEAN RECORD		SNR20		SNR15	
	FA	DD	FA	DD	FA	DD
Algorithm II.1 + polynomials	0	12.7 ± 18.8	0	20.3 ± 17.9	1	9.2 ± 11.0
Algorithm II.1 + neural networks	1	2.5 ± 2.4	0	15.2 ± 21.4	1	8.3 ± 2.7
Algorithm IV.1	1	3.2 ± 6.2	0	18.5 ± 19.7	1	12.5 ± 8.9
KLIEP	0	10.3 ± 19.2	0	21.0 ± 21.2	0	20.5 ± 21.6
M-statistic	0	7.3 ± 13.1	0	17.3 ± 20.1	0	14.8 ± 19.4

C. Univariate data II: Sberbank shares analysis

To provide more experiments on real-world time series we tested the algorithm performance on dataset of Sberbank shares collected in the period from 23/05/2013 to 23/05/2023 with a daily frequency. To eliminate trend component we took first order difference. Change points were annotated manually making use of data plots and information from the open sources. The modified time series with labeled change points is depicted in Figure 5.

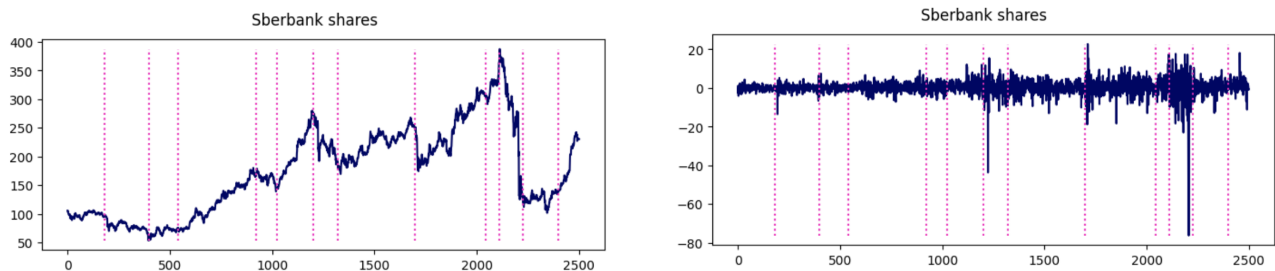


Figure 5. Sberbank shares data set. Left: the original Sberbank shares time series. Right: the time series after preprocessing. The dotted vertical lines correspond to change points.

After preprocessing, we split the data set into training and test parts. The first one was used to tune hyperparameters of the procedures. We set them in a way to ensure that all the competitors have the same number of false alarms on the training set. After that, we applied checked the performance of the methods on the test part and computed average detection delays. The results are presented in Table V and Figure 6.

Table V
THE NUMBER OF FALSE ALARMS (FA) AND THE AVERAGE DETECTION DELAYS (DD) OF ALGORITHM II.1 (WITH TWO VARIANTS OF THE CLASS \mathcal{F}), ALGORITHM IV.1, KLIEP, AND THE KERNEL CHANGE POINT DETECTOR WITH M-STATISTIC ON THE SBERBANK SHARES DATA SET. TWO BEST RESULTS ARE BOLDFACED.

METHOD	β	PARAMETER	FA	DD
Algorithm II.1 + neural networks	5.21	-	2	11.8 ± 12.0
Algorithm II.1 + polynomials	4.4	p = 4	1	9.0 ± 8.5
Algorithm IV.1	2.3	p = 4, $\beta = 0.03$	1	23.8 ± 22.6
M-statistic	1.94	b = 5	2	41.2 ± 30.3
KLIEP	22.93	b = 0.9	2	49.8 ± 40.3

Given that all change points were labeled manually, it is possible that some of them may not have been accurately set, thereby leading to the erroneous detection of mistakes in the performance of methods. To exclude the situation when a false alarm occurs because of inaccurate labeling, we introduced the `min_diff` parameter, which controls the distance between the detected change point and the labeled one. If the change point is detected earlier than the labeled point, but within a distance less than the `min_diff` value, then no false alarm is raised. In such cases, we assumed that the labeled change point was identified with zero delay. What is more, if the algorithm failed to detect the current labeled change point, we assumed that it was identified with a delay equivalent to the difference in positions between the subsequent change point and the current one.

We applied Algorithm II.1 with two variants of the class \mathcal{F} : a class of polynomials of degree 4 and a class of three-layered fully-connected feed-forward neural networks with an architecture (1, 2, 3, 1). Additionally, we applied Algorithm IV.1 with Hermite polynomials of degree 4 and compared results with the KLIEP and the kernel change point detector with M-statistic. According to Table V, we can conclude that the best method for this data set is Algorithm II.1 with polynomial class of \mathcal{F} since it demonstrated the shortest delay and the smallest number of false alarms on the test set. Despite the fact that Algorithm IV.1 with the polynomial reference class \mathcal{F} shows almost the smallest number of false alarms, it has a large detection delay. Although Algorithm II.1 with a neural networks exhibits two false alarms, it is important to note that its detection delay is

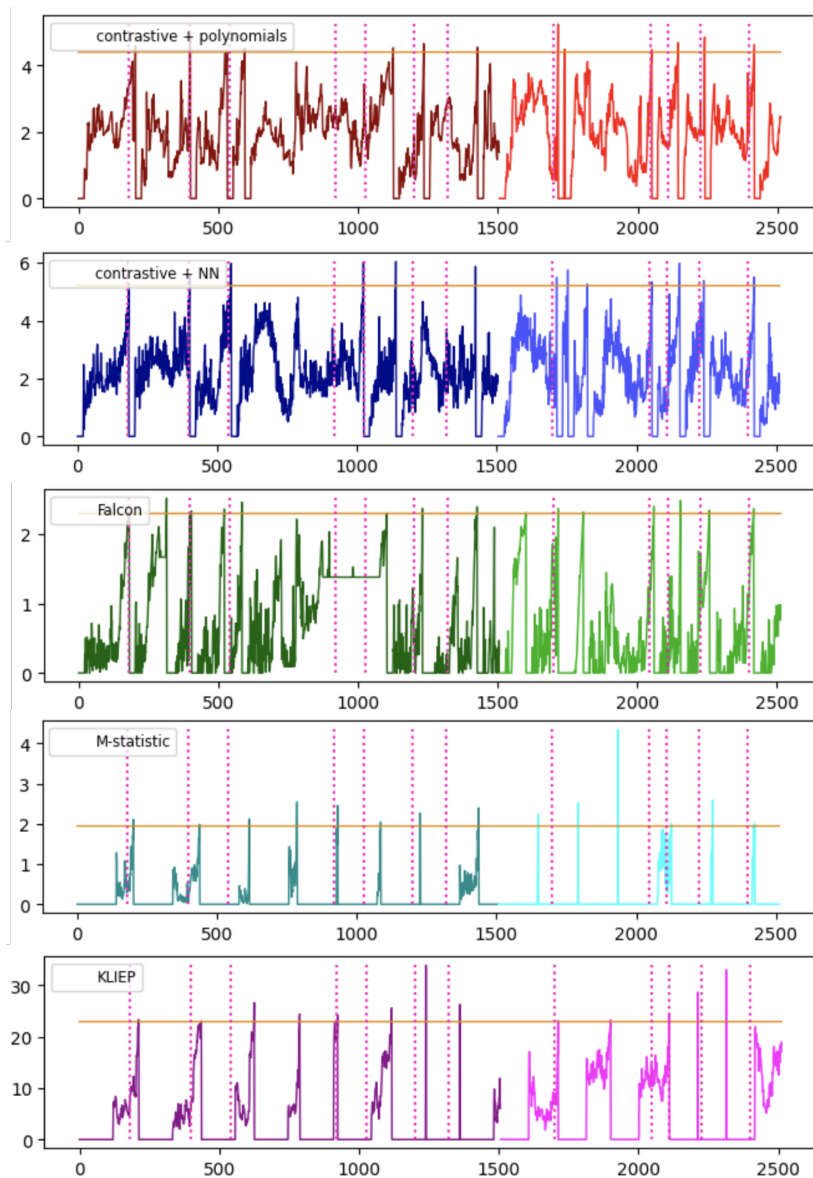


Figure 6. Values of the test statistics for Algorithm II.1 (with two variants of the class \mathcal{F} , red and blue), Algorithm IV.1 (green), the kernel change point detector with M-statistic (cyan) and KLIEP (magenta) in the experiments with Sberbank shares data. The dotted vertical lines and the solid yellow ones correspond to the change points and thresholds, respectively. The dark shades stand for the training period, while the light ones denote the test part.

smaller than the one of the kernel change point detector with M-statistic, as well as of the KLIEP algorithm and of Algorithm IV.1. All the other methods performed slightly worse with a long delay or a high false alarm rate.

D. Multivariate data I: activity change recognition

In this section, we apply Algorithm II.1 to detect changes in a user’s physical activity. In our experiments, we took a part of the data set WISDM [62], containing 3-dimensional measurements of a smartphone accelerometer, measured at a rate 20Hz. We preprocessed the data set, taking only each 20-th observation. Nevertheless, even after such a reduction the length of the time series was over 3000. The observations are displayed in Figure 7. During the measurement period, the user changed a kind of activity 17 times, i.e. the time series contained 17 change points. Our goal was to detect them as soon as possible.

We applied Algorithm II.1 with two variants of the class \mathcal{F} : a class of linear functions and a class of three-layered fully-connected feed-forward neural networks with an architecture (1, 2, 3, 1). We also considered Algorithm IV.1 with a linear class \mathcal{F} . As before, we compared our procedures with KLIEP and the kernel change point detector with M-statistic. The information about thresholds and parameters of the algorithms is collected in Table VI. We split the data set into train and test parts in such a way that the former one contains 8 change points. We set the thresholds as the maximal value of the test statistics on the first four stationary parts of the time series. After that, we computed the average detection delay of each algorithm. The

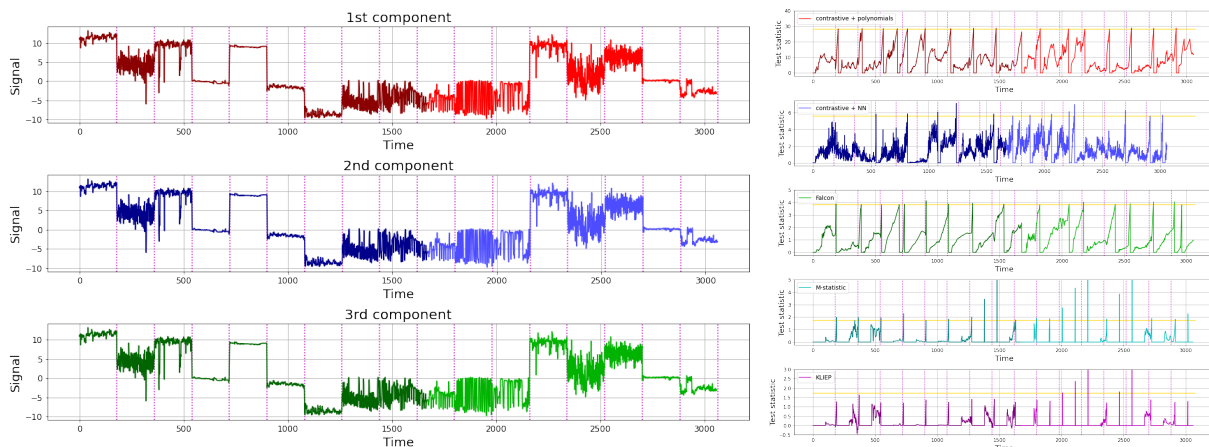


Figure 7. Left: three-dimensional time series from the WISDM data set. Right: the corresponding values of the test statistics for Algorithm II.1 (with two variants of the class \mathcal{F} , red and blue), Algorithm IV.1 (green), the kernel change point detector with M-statistic (cyan) and KLIEP (magenta). The dotted vertical lines and the solid yellow ones correspond to the change points and thresholds, respectively. The dark shades stand for the training period, while the light ones denote the test part.

results are presented in Table VI. The plots of the test statistics are shown in Figure 7. According to Table VI, Algorithm II.1 and Algorithm IV.1 with the class of linear functions outperform the competitors, having a shorter detection delay and a smaller number of false alarms. The best algorithm, Algorithm II.1 with the linear class, does not make false alarms at all.

Table VI
THE NUMBER OF FALSE ALARMS (FA) AND THE AVERAGE DETECTION DELAYS (DD) OF ALGORITHM II.1 (WITH TWO VARIANTS OF THE CLASS \mathcal{F}), KLIEP, AND THE KERNEL CHANGE POINT DETECTOR WITH M-STATISTIC ON THE WISDM DATA SET. TWO BEST RESULTS ARE BOLDFACED.

METHOD	β	PARAMETER	FA	DD
Algorithm II.1 + linear class	28.07	$p = 1$	0	28.3 ± 15.1
Algorithm II.1 + neural networks	5.60	-	2	98.9 ± 52.8
Algorithm IV.1	3.82	$p = 1, \beta = 2.5$	1	30.6 ± 27.7
KLIEP	1.15	$b = 20$	4	30.9 ± 30.1
M-statistic	1.73	$b = 20$	4	30.7 ± 28.2

E. Multivariate data II: room occupancy detection

Finally, we applied Algorithm II.1 and Algorithm IV.1 to detect changes in room occupancy based on Temperature, Humidity, Light, and CO₂ variables. The four-dimensional time series was obtained from UCI repository. The data preprocessing pipeline comprised two sequential steps. Firstly, we selected every 16th observation to reduce the length of the time series. Additionally, we calculated the differences between the logarithms of consecutive observations and normalized these differences by dividing them by the earliest observation. Last transformation aimed to convert the non-stationary time series into a stationary one. After the preprocessing, the time series consisted of roughly 500 data points, with 9 of them labeled as change points. Description of the change point annotation pipeline may be found in [59, Section Annotation Collection]. The time series is displayed in Figure 8 (left).

As a class \mathcal{F} in both Algorithm II.1 and Algorithm IV.1 we took a class of polynomials of degree 1, which entailed the implementation of the algorithm on the original data augmented with an additional column of ones. Additionally, for the Algorithm II.1 we took a class of three-layered fully-connected feed-forward neural networks with an architecture (1, 2, 3, 1) as the class \mathcal{F} . We compared the performance with KLIEP and the kernel change point detector with M-statistic. The algorithm application pipeline was identical to that used for the Sberbank shares data set (see Section V-C). A reader can find bandwidths for KLIEP, M-statistic and thresholds for all methods in Table VII, as well as the number of false alarms and detection delays on the test part. The plots of test statistics are depicted in Figure 8 (right). Remarkably, almost all methods except for FALCON miss the last change point. Despite the fact that KLIEP and M-statistic methods have almost the lowest rate of false alarms, the detection delay on test set is much more longer compared to other methods. The contrastive method with the affine reference class \mathcal{F} demonstrates the shortest delay with a small number of false alarms.

Table VII
 THE NUMBER OF FALSE ALARMS (FA) AND THE AVERAGE DETECTION DELAYS (DD) OF ALGORITHM II.1 (WITH TWO VARIANTS OF THE CLASS \mathcal{F}), ALGORITHM IV.1, KLIEP, AND THE KERNEL CHANGE POINT DETECTOR WITH M-STATISTIC ON THE OCCUPANCY DATA SET. TWO BEST RESULTS ARE BOLDFACED.

METHOD	\hat{j}	PARAMETER	FA	DD
Algorithm II.1 + neural networks	5	-	1	5.75 ± 2.86
Algorithm II.1 + polynomials	0.073	$p = 1$	2	3.50 ± 2.69
Algorithm IV.1	0.404	$p = 1, \beta = 0.073$	2	5.25 ± 7.94
M-statistic	4	$b = 0.2$	1	10.25 ± 5.67
KLIEP	1.66	$b = 0.5$	1	11.25 ± 6.68

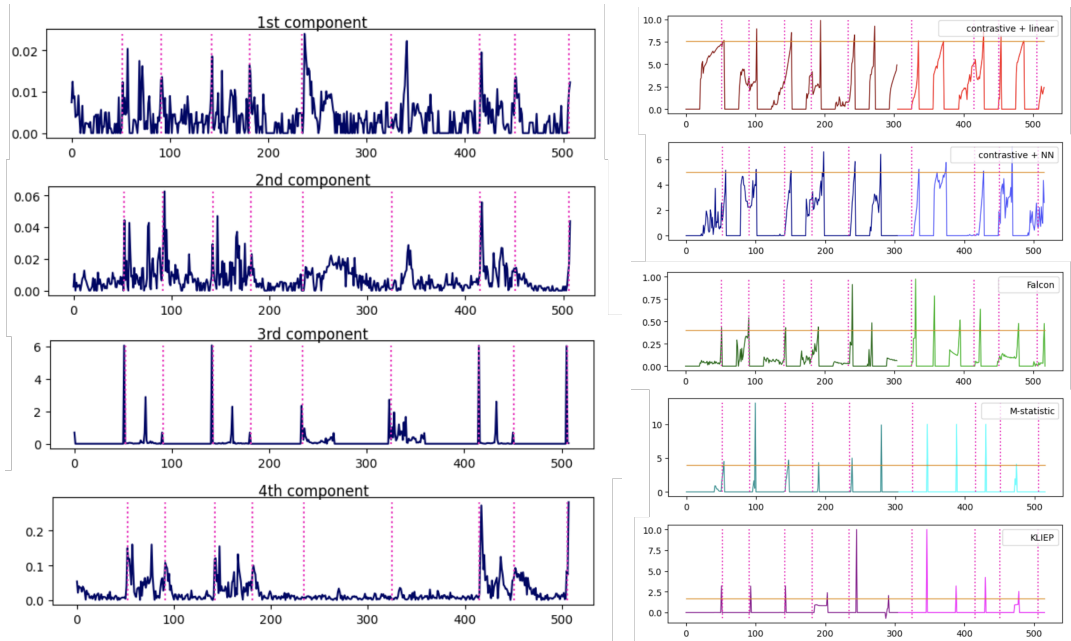


Figure 8. Left: four-dimensional time series from the occupancy data set. Right: the corresponding values of the test statistics for Algorithm II.1 (with two variants of the class \mathcal{F} , red and blue), Algorithm IV.1 (green), the kernel change point detector with M-statistic (cyan) and KLIEP (magenta). The dotted vertical lines and the solid yellow ones correspond to the change points and thresholds, respectively. The dark shades stand for the training period, while the light ones denote the test part.

VI. PROOFS OF THE MAIN RESULTS

This section collects proofs of our main results, presented in Sections II and III.

A. Proof of Lemma II.2

Let

$$D^*(x) = \frac{e^{f^*(x)}}{1 + e^{f^*(x)}} = \frac{p(x)}{p(x) + q(x)}.$$

With the introduced notation, it holds that

$$f^*(x) - \ln\left(\frac{1 + e^{f^*(x)}}{2}\right) = \ln(2D^*(x)) \quad \text{and} \quad -\ln\left(\frac{1 + e^{f^*(x)}}{2}\right) = \ln(2 - 2D^*(x)).$$

If $\tau^* = \tau$, then we obtain that

$$\begin{aligned} \mathbb{E}\mathcal{T}_{\tau,t}(f^*) &= \frac{\tau(t - \tau)}{t} \left[\int \ln(2D^*(x))p(x)dm + \int \ln(2 - 2D^*(x))q(x)dm \right] \\ &= \frac{\tau(t - \tau)}{t} \left[\int \ln\left(\frac{2p(x)}{p(x) + q(x)}\right)p(x)dm + \int \ln\left(\frac{2q(x)}{p(x) + q(x)}\right)q(x)dm \right] \\ &= \frac{2\tau(t - \tau)}{t} \left[\text{KL}\left(p, \frac{p+q}{2}\right) + \text{KL}\left(q, \frac{p+q}{2}\right) \right] \\ &\equiv \frac{2\tau(t - \tau)}{t} \text{JS}(p, q). \end{aligned}$$

Fix a function f , introduce $D(x) = e^{f(x)}/(1 + e^{f(x)})$ and note that

$$\begin{aligned} \mathbb{E}\mathcal{T}_{\tau,t}(f^*) - \mathbb{E}\mathcal{T}_{\tau,t}(f) &= \frac{\tau(t-\tau)}{t} \left[\int \ln \left(\frac{D^*(x)}{D(x)} \right) \mathfrak{p}(x) \mathrm{d}\mathbf{m} + \int \ln \left(\frac{1-D^*(x)}{1-D(x)} \right) \mathfrak{q}(x) \mathrm{d}\mathbf{m} \right] \\ &= \frac{\tau(t-\tau)}{t} \left[\int D^*(x) \ln \left(\frac{D^*(x)}{D(x)} \right) (\mathfrak{p}(x) + \mathfrak{q}(x)) \mathrm{d}\mathbf{m} \right. \\ &\quad \left. + \int (1-D^*(x)) \ln \left(\frac{1-D^*(x)}{1-D(x)} \right) (\mathfrak{p}(x) + \mathfrak{q}(x)) \mathrm{d}\mathbf{m} \right]. \end{aligned}$$

Substituting $D^*(x)$ and $D(x)$ by $e^{f^*(x)}/(1 + e^{f^*(x)})$ and $1/(1 + e^{f^*(x)})$, respectively, we obtain that

$$\begin{aligned} \mathbb{E}\mathcal{T}_{\tau,t}(f^*) - \mathbb{E}\mathcal{T}_{\tau,t}(f) &= \frac{\tau(t-\tau)}{t} \left[\int \frac{e^{f^*(x)}}{1 + e^{f^*(x)}} (f^*(x) - f(x)) (\mathfrak{p}(x) + \mathfrak{q}(x)) \mathrm{d}\mathbf{m} \right] \\ &\quad - \frac{\tau(t-\tau)}{t} \left[\int \frac{e^{f^*(x)}}{1 + e^{f^*(x)}} \ln \left(\frac{1 + e^{f^*(x)}}{1 + e^{f(x)}} \right) (\mathfrak{p}(x) + \mathfrak{q}(x)) \mathrm{d}\mathbf{m} \right] \\ &\quad - \frac{\tau(t-\tau)}{t} \left[\int \frac{1}{1 + e^{f^*(x)}} \ln \left(\frac{1 + e^{f^*(x)}}{1 + e^{f(x)}} \right) (\mathfrak{p}(x) + \mathfrak{q}(x)) \mathrm{d}\mathbf{m} \right] \\ &= \frac{\tau(t-\tau)}{t} \left[\int \frac{e^{f^*(x)}}{1 + e^{f^*(x)}} (f^*(x) - f(x)) (\mathfrak{p}(x) + \mathfrak{q}(x)) \mathrm{d}\mathbf{m} \right] \\ &\quad - \frac{\tau(t-\tau)}{t} \left[\int \ln \left(\frac{1 + e^{f^*(x)}}{1 + e^{f(x)}} \right) (\mathfrak{p}(x) + \mathfrak{q}(x)) \mathrm{d}\mathbf{m} \right]. \end{aligned} \tag{13}$$

Consider a function $g : \mathbb{R}^2 \rightarrow \mathbb{R}$, defined as

$$g(u, v) = \frac{(u-v)e^u}{1+e^u} - \ln \left(\frac{1+e^u}{1+e^v} \right).$$

Note that, for any $u, v \in \mathbb{R}$, we have $g(u, u) = 0$,

$$\left. \frac{\partial g(u, v)}{\partial v} \right|_{v=u} = \left[-\frac{e^u}{1+e^u} + \frac{e^v}{1+e^v} \right] \Big|_{v=u} = 0, \quad \text{and} \quad \frac{\partial^2 g(u, v)}{\partial v^2} = \frac{e^v}{(1+e^v)^2} \leq \frac{1}{4}.$$

Hence, for any $u, v \in \mathbb{R}$, it holds that

$$g(u, v) \leq \frac{(u-v)^2}{8}.$$

Applying this inequality to the right-hand side of (13), we obtain that

$$\begin{aligned} \mathbb{E}\mathcal{T}_{\tau,t}(f^*) - \mathbb{E}\mathcal{T}_{\tau,t}(f) &\leq \frac{\tau(t-\tau)}{8t} \left[\int (f^*(x) - f(x))^2 (\mathfrak{p}(x) + \mathfrak{q}(x)) \mathrm{d}\mathbf{m} \right] \\ &\leq \frac{\tau(t-\tau)}{8t} \left(\|f^* - f\|_{L_2(\mathfrak{p})}^2 + \|f^* - f\|_{L_2(\mathfrak{q})}^2 \right). \end{aligned}$$

Taking into account that $\mathbb{E}\mathcal{T}_{\tau,t}(f^*) = 2\tau(t-\tau) \text{JS}(\mathfrak{p}, \mathfrak{q})/t$, we finally get

$$\mathbb{E}\mathcal{T}_{\tau,t}(f) \geq \frac{2\tau(t-\tau)}{t} \left(\text{JS}(\mathfrak{p}, \mathfrak{q}) - \frac{1}{16} \|f - f^*\|_{L_2(\mathfrak{p})}^2 - \frac{1}{16} \|f - f^*\|_{L_2(\mathfrak{q})}^2 \right).$$

B. Proof of Theorem II.4

Lemma VI.1. *Let a function f take its values in $[-B, B]$. Assume that X_1, \dots, X_t are independent and identically distributed. Then, for any $\tau \in \{1, \dots, t-1\}$, it holds that*

$$\frac{\tau(t-\tau) \mathbb{E}f^2(X_1)}{t} \leq \frac{-\mathbb{E}\mathcal{T}_{\tau,t}(f)}{\varkappa}.$$

where $\mathcal{T}_{\tau,t}(f)$ is defined in (4) and

$$\varkappa = \min \left\{ \frac{e^B}{(1+e^B)^2}, \frac{e^{-B}}{(1+e^{-B})^2} \right\}.$$

Moreover, we have $\text{Var}(\mathcal{T}_{\tau,t}(f)) \leq \tau(t-\tau) \mathbb{E}f^2(X_1)/t \leq -\mathbb{E}\mathcal{T}_{\tau,t}(f)/\varkappa$.

In the proof of Theorem II.4, we use an approach based on local Rademacher complexities (see, for instance, [2]). The inequality $\text{Var}(\mathcal{T}_{\tau,t}(f)) \leq -\mathbb{E}\mathcal{T}_{\tau,t}(f)/\varkappa$ will allow us to get the so-called fast rates of convergence. However, note that

$$\frac{t-\tau}{t} \sum_{s=1}^{\tau} \left[f(X_s) - \ln \left(\frac{1+e^{f(X_s)}}{2} \right) \right] \quad \text{nor} \quad \frac{\tau}{t} \sum_{s=\tau+1}^t \ln \left(\frac{1+e^{f(X_s)}}{2} \right)$$

do not have the properties of $\mathcal{T}_{\tau,t}(f)$, discussed in Lemma VI.1. This means that, in order to exploit the curvature of $\mathbb{E}\mathcal{T}_{\tau,t}(f)$ with respect to f , we must study both terms in (4) simultaneously. The problem is that the terms in the right-hand side of (4) are not identically distributed (though independent). We must slightly modify the argument of [2] to overcome this issue.

Introduce a parameter $r > 0$ to be specified later. For any $f \in \mathcal{F}$, define

$$k(f) = \min \left\{ m \in \mathbb{Z}_+ : 4^m r \geq \frac{\tau(t-\tau)}{t} \mathbb{E}f^2(X_1) \right\}$$

and consider the empirical process $4^{-k(f)}\mathcal{T}_{\tau,t}(f)$, $f \in \mathcal{F}$. The next lemma allows us to bound the expectation of

$$\sup_{f \in \mathcal{F}} \left[4^{-k(f)}\mathcal{T}_{\tau,t}(f) - \mathbb{E}4^{-k(f)}\mathcal{T}_{\tau,t}(f) \right].$$

Lemma VI.2. *Grant Assumption II.3. Then there exists an absolute constant $C > 0$ such that*

$$\begin{aligned} & \mathbb{E} \sup_{f \in \mathcal{F}} \left[4^{-k(f)}\mathcal{T}_{\tau,t}(f) - \mathbb{E}4^{-k(f)}\mathcal{T}_{\tau,t}(f) \right] \\ & \leq C \left(\sqrt{rd \log \left(\frac{A\tau(t-\tau)}{rt} \right)} + Bd \log \left(\frac{A\tau(t-\tau)}{rt} \right) \right) \end{aligned} \quad (14)$$

The proof of Lemma VI.2 is based on the bracketing entropy chaining argument [22, Lemma 7]. Denote the right-hand side of (14) by $\Phi(r)$. Talagrand's concentration inequality [32, Theorem 1.1], combined with the result of Lemma VI.2, yields that

$$\sup_{f \in \mathcal{F}} \left[4^{-k(f)}\mathcal{T}_{\tau,t}(f) - \mathbb{E}4^{-k(f)}\mathcal{T}_{\tau,t}(f) \right] \leq 2\Phi(r) + \sqrt{2r \log(1/\delta)} + 4B \log(1/\delta)$$

on an event E_1 , such that $\mathbb{P}(E_1) \geq 1 - \delta$. Here we used the fact that, for any $f \in \mathcal{F}$, it holds that

$$\text{Var} \left(4^{-k(f)}\mathcal{T}_{\tau,t}(f) \right) = \frac{1}{16^{k(f)}} \text{Var}(\mathcal{T}_{\tau,t}(f)) \leq \frac{\tau(t-\tau)}{4^{k(f)}t} \mathbb{E}f^2(X_1) \leq r.$$

Take

$$r = \max \left\{ \frac{128Cd}{\varkappa} \left(\frac{4Cd}{\varkappa} \vee B \right) \log \left(\frac{A\tau(t-\tau)\varkappa}{16Ctd(B \wedge 4Cd/\varkappa)} \right), \left(\frac{8}{\varkappa} \vee B \right) \frac{16 \log(1/\delta)}{\varkappa} \right\} \quad (15)$$

and consider two cases. For all functions $f \in \mathcal{F}$, satisfying the inequality $\tau(t-\tau)\mathbb{E}f^2(X_1) \leq rt$, we have $k(f) = 0$ and then, on the event E_1 , it holds that

$$\begin{aligned} \mathcal{T}_{\tau,t}(f) & \leq \mathbb{E}\mathcal{T}_{\tau,t}(f) + 2\Phi(r) + \sqrt{2r \log(1/\delta)} + 4B \log(1/\delta) \\ & \leq 2\Phi(r) + \sqrt{2r \log(1/\delta)} + 4B \log(1/\delta) \\ & \lesssim \frac{d}{\varkappa} \log \left(\frac{A\varkappa^2\tau(t-\tau)}{td} \right) + Bd \log \left(\frac{A\varkappa\tau(t-\tau)}{tBd} \right) + \left(\frac{1}{\varkappa} \vee B \right) \log(1/\delta). \end{aligned}$$

Here we used the fact that $\mathbb{E}\mathcal{T}_{\tau,t}(f) \leq 0$ for all $f \in \mathcal{F}$ (follows from Lemma VI.1). Otherwise, due to the definition of $k(f)$, it holds that

$$\frac{-\mathbb{E}\mathcal{T}_{\tau,t}(f)}{\varkappa} \geq \frac{\tau(t-\tau)\mathbb{E}f^2(X_1)}{t} \geq 4^{k(f)-1}r$$

and, hence,

$$\mathcal{T}_{\tau,t}(f) \leq 4^{k(f)} \left(-\frac{\varkappa r}{4} + 2\Phi(r) + \sqrt{2r \log(1/\delta)} + 4B \log(1/\delta) \right)$$

on E_1 . For r given by (15), we have

$$-\frac{\varkappa r}{16} \geq \max \left\{ \Phi(r), \sqrt{2r \log(1/\delta)}, 4B \log(1/\delta) \right\}.$$

Thus, we obtain that $\mathcal{T}_{\tau,t}(f) \leq 0$ on E_1 for all $f \in \mathcal{F}$ such that $k(f) \geq 1$. Hence, with probability at least $1 - \delta$,

$$\sup_{f \in \mathcal{F}} \mathcal{T}_{\tau,t}(f) \lesssim \frac{d}{\varkappa} \log \left(\frac{A\varkappa^2\tau(t-\tau)}{td} \right) + Bd \log \left(\frac{A\varkappa\tau(t-\tau)}{tBd} \right) + \left(\frac{1}{\varkappa} \vee B \right) \log(1/\delta).$$

The expression in the right-hand side can be simplified if one takes into account that $\varkappa \geq 0.5e^{-B}$:

$$\sup_{f \in \mathcal{F}} \mathcal{T}_{\tau,t}(f) \lesssim de^B \left[B + \log \left(\frac{A\tau(t-\tau)}{td} \right) \right] + e^B \log(1/\delta).$$

C. Proof of Theorem II.7

As in the proof of Theorem II.4, we use the peeling and reweighting argument. Introduce a parameter $r > 0$ to be specified later. Recall that, for any $f \in \mathcal{F}$,

$$k(f) = \min \left\{ m \in \mathbb{Z}_+ : 4^m r \geq \frac{\tau(t-\tau)}{t} \mathbb{E} f^2(X_1) \right\},$$

and, for any $b \geq a > 0$, define

$$\mathcal{F}(a, b) = \left\{ f \in \mathcal{F} : \frac{at}{\tau(t-\tau)} \leq \mathbb{E} f^2(X_1) \leq \frac{bt}{\tau(t-\tau)} \right\}.$$

Then it holds that

$$\begin{aligned} & \sup_{f \in \mathcal{F}} \left[4^{-k(f)} \mathcal{T}_{\tau,t}(f) - \mathbb{E} 4^{-k(f)} \mathcal{T}_{\tau,t}(f) \right] \\ & \leq \max \left\{ \sup_{f \in \mathcal{F}(0,r)} \left[4^{-k(f)} \mathcal{T}_{\tau,t}(f) - \mathbb{E} 4^{-k(f)} \mathcal{T}_{\tau,t}(f) \right], \right. \\ & \quad \left. \max_{j \in \mathbb{Z}_+} \sup_{f \in \mathcal{F}(4^j r, 4^{j+1} r)} \left[4^{-k(f)} \mathcal{T}_{\tau,t}(f) - \mathbb{E} 4^{-k(f)} \mathcal{T}_{\tau,t}(f) \right] \right\} \\ & \leq \max_{j \in \mathbb{Z}_+} \left\{ 4^{-j+1} \sup_{f \in \mathcal{F}(0, 4^j r)} \left[\mathcal{T}_{\tau,t}(f) - \mathbb{E} \mathcal{T}_{\tau,t}(f) \right] \right\}. \end{aligned}$$

Fix any $f, g \in \mathcal{F}$. Due to the centering lemma [60, Lemma 2.6.8] (see also the inequality (22)), it holds that

$$\| \mathcal{T}_{\tau,t}(f) - \mathbb{E} \mathcal{T}_{\tau,t}(f) - \mathcal{T}_{\tau,t}(g) + \mathbb{E} \mathcal{T}_{\tau,t}(g) \|_{\psi_2} \lesssim \| \mathcal{T}_{\tau,t}(f) - \mathcal{T}_{\tau,t}(g) \|_{\psi_2}.$$

since the probability measure is clear from context, we write ψ_2 , instead of $\psi_2(\mathbf{p})$, in this proof to avoid the abuse of notation. For any $f \in \mathcal{F}$, let us represent

$$\mathcal{T}_{\tau,t}(f) = \frac{\tau(t-\tau)}{t} \mathcal{P}_{\tau,t}(f) + \frac{\tau(t-\tau)}{t} \mathcal{Q}_{\tau,t}(f),$$

where

$$\mathcal{P}_{\tau,t}(f) = \frac{1}{\tau} \sum_{s=1}^{\tau} \left[f(X_s) - \ln \left(\frac{1 + e^{f(X_s)}}{2} \right) \right]$$

and

$$\mathcal{Q}_{\tau,t}(f) = -\frac{1}{t-\tau} \sum_{s=\tau+1}^t \ln \left(\frac{1 + e^{f(X_s)}}{2} \right).$$

The triangle inequality yields that

$$\| \mathcal{T}_{\tau,t}(f) - \mathcal{T}_{\tau,t}(g) \|_{\psi_2} \leq \frac{\tau(t-\tau)}{t} \| \mathcal{P}_{\tau,t}(f) - \mathcal{P}_{\tau,t}(g) \|_{\psi_2} + \frac{\tau(t-\tau)}{t} \| \mathcal{Q}_{\tau,t}(f) - \mathcal{Q}_{\tau,t}(g) \|_{\psi_2}.$$

Applying Proposition A.1 to $\mathcal{P}_{\tau,t}(f) - \mathcal{P}_{\tau,t}(g)$ and $\mathcal{Q}_{\tau,t}(f) - \mathcal{Q}_{\tau,t}(g)$, we obtain that

$$\| \mathcal{P}_{\tau,t}(f) - \mathcal{P}_{\tau,t}(g) \|_{\psi_2} \lesssim \frac{1}{\sqrt{\tau}} \left\| \ln \left(\frac{e^{f(X_1)}}{1 + e^{f(X_1)}} \right) - \ln \left(\frac{e^{g(X_1)}}{1 + e^{g(X_1)}} \right) \right\|_{\psi_2}$$

and

$$\| \mathcal{Q}_{\tau,t}(f) - \mathcal{Q}_{\tau,t}(g) \|_{\psi_2} \lesssim \frac{1}{\sqrt{t-\tau}} \left\| \ln \left(1 + e^{f(X_1)} \right) - \ln \left(1 + e^{g(X_1)} \right) \right\|_{\psi_2}.$$

Moreover, since the maps $y \mapsto (y - \log(1 + e^y))$ and $y \mapsto \log(1 + e^y)$ are 1-Lipschitz, we have

$$\left\| \ln \left(\frac{e^{f(X_1)}}{1 + e^{f(X_1)}} \right) - \ln \left(\frac{e^{g(X_1)}}{1 + e^{g(X_1)}} \right) \right\|_{\psi_2} \leq \| f - g \|_{\psi_2}$$

and, similarly,

$$\left\| \ln \left(1 + e^{f(X_1)} \right) - \ln \left(1 + e^{g(X_1)} \right) \right\|_{\psi_2} \leq \| f - g \|_{\psi_2}.$$

Hence,

$$\begin{aligned} \|\mathcal{T}_{\tau,t}(f) - \mathcal{T}_{\tau,t}(g)\|_{\psi_2} &\lesssim \left(\frac{(t-\tau)\sqrt{\tau}}{t} + \frac{\tau\sqrt{t-\tau}}{t} \right) \|f - g\|_{\psi_2} \\ &\lesssim \sqrt{\frac{t}{\tau(t-\tau)}} \|f - g\|_{\psi_2} \\ &\leq L \sqrt{\frac{t}{\tau(t-\tau)}} \|f - g\|_{L_2(\mathfrak{p})}, \end{aligned}$$

and we can apply a corollary of [35, Theorem 11.2 and eq. (11.3)] (see the discussion in [35, Theorem p. 302]): for any $j \in \mathbb{Z}_+$, it holds that

$$\begin{aligned} &\left\| \sup_{f \in \mathcal{F}(0, 4^j r)} [\mathcal{T}_{\tau,t}(f) - \mathbb{E}\mathcal{T}_{\tau,t}(f)] \right\|_{\psi_2} \\ &\lesssim L \sqrt{\frac{t}{\tau(t-\tau)}} \int_0^{\mathcal{D}(\mathcal{F}(0, 4^j r), L_2(\mathfrak{p}))} \sqrt{\log \mathcal{N}(\mathcal{F}(0, 4^j r), L_2(\mathfrak{p}), u)} du \\ &\leq L \sqrt{\frac{t}{\tau(t-\tau)}} \int_0^{4^j r t / \tau / (t-\tau)} \sqrt{d \log \left(\frac{A}{\varepsilon} \right)} du \\ &\lesssim L \sqrt{4^j r d \log \left(\frac{A\tau(t-\tau)}{4^j r t} \right)}. \end{aligned}$$

This and (20) imply that, for any $\delta \in (0, 1)$ and for any $j \in \mathbb{Z}_+$, with probability at least $1 - 2^{-j-1}\delta$, it holds that

$$\sup_{f \in \mathcal{F}(0, 4^j r)} [\mathcal{T}_{\tau,t}(f) - \mathbb{E}\mathcal{T}_{\tau,t}(f)] \lesssim L \sqrt{4^j r d \log \left(\frac{A\tau(t-\tau)}{4^j r t} \right) \log \left(\frac{2^{j+2}}{\delta} \right)}.$$

Applying the union bound, we obtain that, for any $\delta \in (0, 1)$, with probability at least $1 - \delta$,

$$\begin{aligned} \sup_{f \in \mathcal{F}} \left[4^{-k(f)} \mathcal{T}_{\tau,t}(f) - \mathbb{E} 4^{-k(f)} \mathcal{T}_{\tau,t}(f) \right] &\leq \max_{j \in \mathbb{Z}_+} \left\{ 4^{-j+1} \sup_{f \in \mathcal{F}(0, 4^j r)} [\mathcal{T}_{\tau,t}(f) - \mathbb{E}\mathcal{T}_{\tau,t}(f)] \right\} \\ &\lesssim \max_{j \in \mathbb{Z}_+} \left\{ 2^{-j} L \sqrt{r d \log \left(\frac{A\tau(t-\tau)}{4^j r t} \right) \log \left(\frac{2^{j+2}}{\delta} \right)} \right\} \\ &\lesssim L \sqrt{r d \log \left(\frac{A\tau(t-\tau)}{r t} \right) \log(1/\delta)}. \end{aligned} \tag{16}$$

Let C be a hidden constant in (16) and take

$$r = \frac{16C^2 L^2 d}{\kappa^2} \log \left(\frac{A\kappa^2 \tau(t-\tau)}{16C^2 L^2 t d} \right) \log(1/\delta).$$

From now on, we restrict our attention on an event E_2 , where (16) holds. As in the proof of Theorem II.4, consider two cases. First, if a function $f \in \mathcal{F}$ satisfies $\tau(t-\tau)\mathbb{E}f^2(X_1) \leq r t$, then $k(f) = 0$ and, hence,

$$\begin{aligned} \mathcal{T}_{\tau,t}(f) &\leq \mathcal{T}_{\tau,t}(f) - \mathbb{E}\mathcal{T}_{\tau,t}(f) \lesssim L \sqrt{r d \log \left(\frac{A\tau(t-\tau)}{r t} \right) \log(1/\delta)} \\ &\lesssim \frac{L^2 d}{\kappa} \log \left(\frac{A\kappa^2 \tau(t-\tau)}{L^2 t d} \right) \log(1/\delta). \end{aligned}$$

On the other hand, the inequality $k(f) \geq 1$ means that $\tau(t-\tau)\mathbb{E}f^2(X_1) \geq 4^{k(f)-1} r t$. The next lemma relates the expectations of $f^2(X_1)$ and $\mathcal{T}_{\tau,t}(f)$.

Lemma VI.3. *Assume that a function class \mathcal{F} is L -sub-Gaussian with respect to $X_1 \sim \mathfrak{p}$. Fix any $t \in \mathbb{N}$, $\tau \in \{1, \dots, t-1\}$ and let X_2, \dots, X_t be i.i.d. copies of X_1 . Then, for any $f \in \mathcal{F}$, it holds that*

$$\frac{\tau(t-\tau)}{t} \mathbb{E}f^2(X_1) \leq \frac{-\mathbb{E}\mathcal{T}_{\tau,t}}{\kappa}, \quad \text{where } \kappa = \frac{1}{2} \exp \left\{ -\mathcal{D}(\mathcal{F}, \psi_2) \sqrt{2 \ln(4L\sqrt{2})} \right\}.$$

Lemma VI.3 immediately implies that

$$\frac{4^{-k(f)} \mathbb{E} \mathcal{T}_{\tau,t}}{\kappa} \leq -r/4,$$

and then

$$\mathcal{T}_{\tau,t}(f) \leq -\frac{\kappa r}{4} + CL \sqrt{rd \log \left(\frac{A\tau(t-\tau)}{rt} \right) \log(1/\delta)} \leq 0.$$

Thus, on the event E_2 , it holds that

$$\begin{aligned} \sup_{f \in \mathcal{F}} \mathcal{T}_{\tau,t}(f) &\lesssim \frac{L^2 d}{\kappa} \log \left(\frac{A\kappa^2 \tau(t-\tau)}{L^2 t d} \right) \log(1/\delta) \\ &\lesssim L^2 d e^{\mathcal{D}(\mathcal{F}, \psi_2) \sqrt{2 \log(4L\sqrt{2})}} \left[\mathcal{D}(\mathcal{F}, \psi_2) \sqrt{\log L} + \log \left(\frac{A\tau(t-\tau)}{L^2 t d} \right) \right] \log(1/\delta). \end{aligned}$$

D. Proof of Theorem II.8

Theorem II.4 and the union bound yield that, in the stationary regime, with probability at least $1 - \delta$

$$\max_{1 \leq t \leq T} \mathcal{S}_t \leq C d e^B \left[B + \log \left(\frac{AT}{d} \right) \right] + C e^B \log(T/\delta),$$

where C is an absolute positive constant. Hence, if X_1, \dots, X_T are i.i.d. random elements and

$$\mathfrak{z} = C d e^B \left[B + \log \left(\frac{AT}{d} \right) \right] + C e^B \log(T/\delta),$$

then Algorithm II.1 does not stop on the first T iterations with probability at least $1 - \delta$.

On the other hand, let $f^\circ \in \operatorname{argmin}_{f \in \mathcal{F}} \|f - \log(\mathbf{p}/\mathbf{q})\|_{L_2(\mathbf{p}+\mathbf{q})}$. Bernstein's inequality implies that, for any fixed $t \in \mathbb{N}$, with probability at least $1 - \delta$,

$$\begin{aligned} \mathcal{T}_{\tau^*,t}(f^\circ) &> \mathbb{E} \mathcal{T}_{\tau^*,t}(f^\circ) - \sqrt{2 \operatorname{Var}(\mathcal{T}_{\tau^*,t}(f^\circ)) \log(1/\delta)} - 3B \log(1/\delta) \\ &> \frac{2\tau^*(t-\tau^*)}{t} \left(\operatorname{JS}(\mathbf{p}, \mathbf{q}) - \frac{\rho^2(\mathcal{F})}{16} \right) - B \left(\sqrt{\frac{2(t-\tau^*)\tau^* \log(1/\delta)}{t}} + 3 \log(1/\delta) \right). \end{aligned}$$

Here we used the fact that $\log((1+e^u)/2) \leq |u|$ for all $u \in \mathbb{R}$, which yields

$$\begin{aligned} \operatorname{Var}(\mathcal{T}_{\tau^*,t}(f^\circ)) &\leq \frac{(t-\tau^*)^2 \tau^*}{t} \mathbb{E} \log^2 \left(\frac{2e^{f^\circ(X_1)}}{1+e^{f^\circ(X_1)}} \right) + \frac{(t-\tau^*)\tau^{*2}}{t} \mathbb{E} \log^2 \left(\frac{2}{1+e^{f^\circ(X_1)}} \right) \\ &\leq \frac{(t-\tau^*)^2 \tau^*}{t} \mathbb{E} (f^\circ(X_1))^2 + \frac{(t-\tau^*)\tau^{*2}}{t} \mathbb{E} (f^\circ(X_1))^2 \\ &\leq \frac{B^2(t-\tau^*)\tau^*}{t}. \end{aligned}$$

Let t° be the smallest positive integer, satisfying the inequality

$$\frac{\tau^*(t-\tau^*)}{t} \geq \frac{\tau_{\min}}{2},$$

where

$$\frac{\tau_{\min}}{2} = \left\lceil \frac{B^2 \log(1/\delta)}{2(\operatorname{JS}(\mathbf{p}, \mathbf{q}) - \rho^2(\mathcal{F})/16)^2} + \frac{3B \log(1/\delta) + \mathfrak{z}}{2(\operatorname{JS}(\mathbf{p}, \mathbf{q}) - \rho^2(\mathcal{F})/16)} \right\rceil + 1.$$

Then, with probability at least $1 - \delta$, we have

$$\begin{aligned} \mathcal{S}_{t^\circ} &\geq \mathcal{T}_{\tau^*,t^\circ}(f^\circ) \\ &> \frac{2\tau^*(t-\tau^*)}{t} \left(\operatorname{JS}(\mathbf{p}, \mathbf{q}) - \frac{\rho^2(\mathcal{F})}{16} \right) - B \left(\sqrt{\frac{2(t-\tau^*)\tau^* \log(1/\delta)}{t}} + 3 \log(1/\delta) \right) \\ &\geq \mathfrak{z}. \end{aligned}$$

Thus, on this event, the stopping time of Algorithm II.1 does not exceed t° . This implies that

$$\frac{\tau^*(\hat{t}-\tau^*)}{\hat{t}} \leq \frac{\tau^*(t^\circ+1-\tau^*)}{t^\circ+1} < \frac{\tau_{\min}}{2}.$$

Note that, due to the conditions of Theorem II.8, it holds that $\tau^* \geq \tau_{\min}$. Hence, with probability at least $1 - \delta$,

$$\hat{t} - \tau^* \leq \frac{\tau_{\min} \tau^*}{2(\tau^* - \tau_{\min}/2)} \leq \tau_{\min} \lesssim \frac{B^2 \log(1/\delta)}{(\operatorname{JS}(\mathbf{p}, \mathbf{q}) - \rho^2(\mathcal{F})/16)^2} + \frac{B \log(1/\delta) + \mathfrak{z}}{\operatorname{JS}(\mathbf{p}, \mathbf{q}) - \rho^2(\mathcal{F})/16}.$$

E. Proof of Theorem II.10

The proof of Theorem II.10 is similar to the one of Theorem II.8 but relies on II.7, rather than on II.4. Theorem II.7 and the union bound imply that, in the stationary regime, there exists such $C > 0$ that, with probability at least $1 - \delta$,

$$\max_{1 \leq t \leq T} \mathcal{S}_t \leq CL^2 de^{\mathcal{D}(\mathcal{F}, \psi_2(\mathbf{p}))\sqrt{2\log(4L\sqrt{2})}} \left[\mathcal{D}(\mathcal{F}, \psi_2(\mathbf{p}))\sqrt{\log L} + \log \left(\frac{A\tau(t-\tau)}{L^2td} \right) \right] \log(T/\delta).$$

Hence, if

$$\mathfrak{z} = CL^2 de^{\mathcal{D}(\mathcal{F}, \psi_2(\mathbf{p}))\sqrt{2\log(4L\sqrt{2})}} \left[\mathcal{D}(\mathcal{F}, \psi_2(\mathbf{p}))\sqrt{\log L} + \log \left(\frac{A\tau(t-\tau)}{L^2td} \right) \right] \log(T/\delta),$$

then the running length of Algorithm II.1 exceeds T with probability at least $1 - \delta$.

On the other hand, due to (20), for $f^\circ \in \operatorname{argmin}_{f \in \mathcal{F}} \|f - \log(\mathbf{p}/\mathbf{q})\|_{L_2(\mathbf{p}+\mathbf{q})}$ and any $t \in \mathbb{N}$, with probability at least $1 - \delta$, it holds that

$$\mathcal{T}_{\tau^*,t}(f^\circ) - \mathbb{E}\mathcal{T}_{\tau^*,t}(f^\circ) > -\|\mathcal{T}_{\tau^*,t}(f^\circ) - \mathbb{E}\mathcal{T}_{\tau^*,t}(f^\circ)\|_{\psi_2} \sqrt{\log \frac{2}{\delta}}.$$

According to Proposition A.1 and (22),

$$\begin{aligned} & \|\mathcal{T}_{\tau^*,t}(f^\circ) - \mathbb{E}\mathcal{T}_{\tau^*,t}(f^\circ)\|_{\psi_2} \lesssim \|\mathcal{T}_{\tau^*,t}(f^\circ)\|_{\psi_2} \\ & \lesssim \frac{(t-\tau^*)\tau^*}{t} \left(\frac{1}{\sqrt{\tau^*}} \left\| \ln \left(\frac{2e^{f^\circ}}{1+e^{f^\circ}} \right) \right\|_{\psi_2(\mathbf{p})} + \frac{1}{\sqrt{t-\tau^*}} \left\| \ln \left(\frac{1+e^{f^\circ}}{2} \right) \right\|_{\psi_2(\mathbf{q})} \right) \\ & \lesssim \sqrt{\frac{(t-\tau^*)\tau^*}{t}} \left(\mathcal{D}(\mathcal{F}, \psi_2(\mathbf{p})) \vee \mathcal{D}(\mathcal{F}, \psi_2(\mathbf{q})) \right). \end{aligned}$$

Hence, there exists an absolute constant $c > 0$ such that, for any $t \in \mathbb{N}$, with probability at least $1 - \delta$,

$$\begin{aligned} \mathcal{S}_t & \geq \mathcal{T}_{\tau^*,t}(f^\circ) > \mathbb{E}\mathcal{T}_{\tau^*,t}(f^\circ) - c\sqrt{\frac{(t-\tau^*)\tau^* \log(1/\delta)}{t}} \left(\mathcal{D}(\mathcal{F}, \psi_2(\mathbf{p})) \vee \mathcal{D}(\mathcal{F}, \psi_2(\mathbf{q})) \right) \\ & \geq \frac{2\tau^*(t-\tau^*)}{t} \left(\operatorname{JS}(\mathbf{p}, \mathbf{q}) - \frac{\rho^2(\mathcal{F})}{16} \right) - c\sqrt{\frac{(t-\tau^*)\tau^* \log(1/\delta)}{t}} \left(\mathcal{D}(\mathcal{F}, \psi_2(\mathbf{p})) \vee \mathcal{D}(\mathcal{F}, \psi_2(\mathbf{q})) \right) \end{aligned}$$

Let t° be the smallest positive integer, satisfying the inequality

$$\frac{\tau^*(t-\tau^*)}{t} \geq \frac{\tau_{\min}}{2},$$

where

$$\frac{\tau_{\min}}{2} = \left\lceil \frac{c^2 [\mathcal{D}(\mathcal{F}, \psi_2(\mathbf{p})) \vee \mathcal{D}(\mathcal{F}, \psi_2(\mathbf{q}))]^2 \log(1/\delta)}{(\operatorname{JS}(\mathbf{p}, \mathbf{q}) - \rho^2(\mathcal{F})/16)^2} + \frac{\mathfrak{z}}{\operatorname{JS}(\mathbf{p}, \mathbf{q}) - \rho^2(\mathcal{F})/16} \right\rceil + 1.$$

Then, with probability at least $1 - \delta$, we have

$$\begin{aligned} \mathcal{S}_{t^\circ} & \geq \mathcal{T}_{\tau^*,t^\circ}(f^\circ) \\ & > \frac{2\tau(t-\tau)}{t} \left(\operatorname{JS}(\mathbf{p}, \mathbf{q}) - \frac{\rho^2(\mathcal{F})}{16} \right) - c\sqrt{\frac{(t-\tau^*)\tau^* \log(1/\delta)}{t}} \left(\mathcal{D}(\mathcal{F}, \psi_2(\mathbf{p})) \vee \mathcal{D}(\mathcal{F}, \psi_2(\mathbf{q})) \right) \\ & \geq \mathfrak{z}. \end{aligned}$$

Thus, on this event, the stopping time of Algorithm II.1 does not exceed t° . This implies that

$$\frac{\tau^*(\hat{t} - \tau^*)}{\hat{t}} \leq \frac{\tau^*(t^\circ + 1 - \tau^*)}{t^\circ + 1} < \frac{\tau_{\min}}{2}.$$

Note that, due to the conditions of Theorem II.10, it holds that $\tau^* \geq \tau_{\min}$. Hence, with probability at least $1 - \delta$,

$$\begin{aligned} \hat{t} - \tau^* & \leq \frac{\tau_{\min}\tau^*}{2(\tau^* - \tau_{\min}/2)} \leq \tau_{\min} \\ & \lesssim \frac{[\mathcal{D}(\mathcal{F}, \psi_2(\mathbf{p})) \vee \mathcal{D}(\mathcal{F}, \psi_2(\mathbf{q}))]^2 \log(1/\delta)}{(\operatorname{JS}(\mathbf{p}, \mathbf{q}) - \rho^2(\mathcal{F})/16)^2} + \frac{\mathfrak{z}}{\operatorname{JS}(\mathbf{p}, \mathbf{q}) - \rho^2(\mathcal{F})/16}. \end{aligned}$$

F. Proof of Corollary III.1

Take the smallest positive integers m, N , satisfying the inequalities

$$3^\beta H N^{-\beta/p} \leq \sqrt{\text{JS}(\mathbf{p}, \mathbf{q})}/2 \quad \text{and} \quad (1 + p^2 + \beta^2)6^p(2H + 1)N2^{-m} \leq \sqrt{\text{JS}(\mathbf{p}, \mathbf{q})}/2,$$

and consider the class $\text{NN}(L, \mathcal{A}, s)$ with

$$L = 8 + (m + 5)(1 + \lceil \log_2(p \vee \beta) \rceil) \tag{17}$$

hidden layers, the architecture

$$\mathcal{A} = (p, 6(\lceil \beta \rceil + p)N, \dots, 6(\lceil \beta \rceil + p)N, 1), \tag{18}$$

and the number of non-zero parameters

$$s = 141(p + \beta + 1)^{3+p}N(m + 6). \tag{19}$$

According to Theorem B.1, there exists $f \in \text{NN}(L, \mathcal{A}, s)$ such that

$$\|f - \ln(\mathbf{p}/\mathbf{q})\|_{L_\infty([0,1]^p)} \leq \sqrt{\text{JS}(\mathbf{p}, \mathbf{q})}.$$

Note that, since $\log(\mathbf{p}/\mathbf{q}) \in \mathcal{H}^\beta([0,1]^p, H)$ the L_∞ -norm of such f does not exceed $H + \sqrt{\text{JS}(\mathbf{p}, \mathbf{q})}$. Thus, $f \in \text{NN}_B(L, \mathcal{A}, s)$ for L, \mathcal{A} , and s , given by (17), (18), (5), respectively, and for any $B > H + \sqrt{\text{JS}(\mathbf{p}, \mathbf{q})}$.

On the other hand, due to Lemma B.2, for any $\varepsilon > 0$, the covering number of $\text{NN}_B(L, \mathcal{A}, s)$ with respect to the L_∞ -norm fulfils

$$\log \mathcal{N}(\text{NN}_B(L, \mathcal{A}, s), L_\infty([0,1]^p), \varepsilon) \leq (s + 1) \log \left(\frac{2(L + 1)p(6\lceil \beta \rceil + 6p)^L N^L}{\varepsilon} \right).$$

Hence, $\text{NN}_B(L, \mathcal{A}, s)$ satisfies (II.3) with $d = s + 1$ and $A = 2(L + 1)p(6\lceil \beta \rceil + 6p)^L N^L$. Taking into account that

$$L \lesssim \log(1/\text{JS}(\mathbf{p}, \mathbf{q})), \quad N \lesssim \text{JS}(\mathbf{p}, \mathbf{q})^{-p/(2\beta)}, \quad s \lesssim \text{JS}(\mathbf{p}, \mathbf{q})^{-p/(2\beta)} \log(1/\text{JS}(\mathbf{p}, \mathbf{q})),$$

and substituting these bounds into Theorem II.8, we obtain that if one chooses \mathfrak{z} according to

$$\mathfrak{z} = \frac{C e^B \log(1/\text{JS}(\mathbf{p}, \mathbf{q})) [B + \log(1/\text{JS}(\mathbf{p}, \mathbf{q})) \log T]}{\text{JS}(\mathbf{p}, \mathbf{q})^{p/(2\beta)}} + C e^B \log(T/\delta)$$

with a proper constant $C > 0$ and runs Algorithm II.1 is run with $\mathcal{F} = \text{NN}_B(L, \mathcal{A}, s)$, where L, \mathcal{A} , and s are defined in (17), (18), and (5), respectively, then, with probability at least $1 - \delta$, its running length in the stationary regime is at least T . Otherwise, if $\tau^* < \infty$, then, with probability at least $1 - \delta$, the stopping time \hat{t} of Algorithm II.1 satisfies

$$\hat{t} - \tau^* \lesssim \frac{e^B \log(1/\text{JS}(\mathbf{p}, \mathbf{q})) [B + \log(1/\text{JS}(\mathbf{p}, \mathbf{q})) \log T]}{\text{JS}(\mathbf{p}, \mathbf{q})^{\frac{2\beta+p}{2\beta}}} + e^B \log(T/\delta) + \frac{B^2 \log(1/\delta)}{\text{JS}(\mathbf{p}, \mathbf{q})^2}.$$

This finishes the proof of Corollary III.1.

G. Proof of Corollary III.2

First, show that $\mathcal{D}(\mathcal{F}_{\text{lin}}, \psi_2(\mathbf{p})) \vee \mathcal{D}(\mathcal{F}_{\text{lin}}, \psi_2(\mathbf{q})) \lesssim \|\Sigma^{-1/2}\mu\|$. Let X_1 be a Gaussian random vector with zero mean and the covariance Σ . Then, for any $w \in \mathbb{R}^p$, such that $\|\Sigma^{1/2}w\| \leq \|\Sigma^{-1/2}\mu\|$, we have $w^\top X_1 \sim \mathcal{N}(0, w^\top \Sigma w)$ and

$$\|w^\top X_1\|_{\psi_2(\mathbf{p})} \lesssim \sqrt{w^\top \Sigma w} \leq \|\Sigma^{-1/2}\mu\|.$$

At the same time, for any $b \in \mathbb{R}$, such that $|b| \leq \mu^\top \Sigma^{-1}\mu$, it holds that

$$\|b\|_{\psi_2(\mathbf{p})} \lesssim \mu^\top \Sigma^{-1}\mu \lesssim \|\Sigma^{-1/2}\mu\|,$$

where the last inequality is due to the fact $\|\Sigma^{-1/2}\mu\| \leq \ln(4/3)$. Hence, by the triangle inequality,

$$\|w^\top X_1 + b\|_{\psi_2(\mathbf{p})} \leq \|w^\top X_1\|_{\psi_2(\mathbf{p})} + \|b\|_{\psi_2(\mathbf{p})} \lesssim \|\Sigma^{-1/2}\mu\|$$

for all $w \in \mathbb{R}^p, b \in \mathbb{R}$, such that $\|\Sigma^{1/2}w\| \leq \|\Sigma^{-1/2}\mu\|, |b| \leq \mu^\top \Sigma^{-1}\mu$. Thus, $\mathcal{D}(\mathcal{F}_{\text{lin}}, \psi_2(\mathbf{p})) \lesssim \|\Sigma^{-1/2}\mu\|$. Similarly, $\mathcal{D}(\mathcal{F}_{\text{lin}}, \psi_2(\mathbf{q})) \lesssim \|\Sigma^{-1/2}\mu\|$.

Second, show that \mathcal{F}_{lin} satisfies Assumption II.6. For any $w_1, w_2 \in \mathbb{R}^p$ and $b_1, b_2 \in \mathbb{R}$, it holds that

$$\|w_1^\top X_1 + b_1 - w_2^\top X_1 - b_2\|_{L_2(\mathbf{p})}^2 = (w_1 - w_2)^\top \Sigma (w_1 - w_2) + \|b_1 - b_2\|^2.$$

This yields that, if \mathcal{W} is an ε -net of the ellipsoid $\{w : \|\Sigma^{1/2}w\| \leq \|\Sigma^{-1/2}\mu\|\}$ and \mathcal{B} is an ε -net of the segment $[-\mu^\top \Sigma^{-1}\mu, \mu^\top \Sigma^{-1}\mu]$, then the set

$$\{f_{w,b}(x) = w^\top x + b : w \in \mathcal{W}, b \in \mathcal{B}\}$$

is an $(\varepsilon\sqrt{2})$ -net of \mathcal{F}_{lin} . Thus, we conclude that $\log \mathcal{N}(\mathcal{F}_{\text{lin}}, L_2(\mathbf{p}), \varepsilon) \lesssim p \log(\mu^\top \Sigma^{-1} \mu / \varepsilon)$ for any $\varepsilon > 0$.

It only remains to show that $\text{JS}(\mathbf{p}, \mathbf{q}) \gtrsim \mu^\top \Sigma^{-1} \mu$. Then, substituting the obtained bounds on $\mathcal{D}(\mathcal{F}_{\text{lin}}, \psi_2(\mathbf{p})) \vee \mathcal{D}(\mathcal{F}_{\text{lin}}, \psi_2(\mathbf{q}))$, $\mathcal{N}(\mathcal{F}_{\text{lin}}, L_2(\mathbf{p}), \varepsilon)$, and $\text{JS}(\mathbf{p}, \mathbf{q})$ into the statement of Theorem II.10, we get the assertion of Corollary III.2.

The rest of this section is devoted to the proof of the inequality $\text{JS}(\mathbf{p}, \mathbf{q}) \gtrsim \mu^\top \Sigma^{-1} \mu$. By the definition of $\text{JS}(\mathbf{p}, \mathbf{q})$,

$$\text{JS}(\mathbf{p}, \mathbf{q}) = \frac{\text{KL}(\mathbf{p}, (\mathbf{p} + \mathbf{q})/2) + \text{KL}(\mathbf{q}, (\mathbf{p} + \mathbf{q})/2)}{2}.$$

Consider the first term:

$$\text{KL}\left(\mathbf{p}, \frac{\mathbf{p} + \mathbf{q}}{2}\right) = \mathbb{E}_{\xi \sim \mathbf{p}} \log \frac{2\mathbf{p}}{\mathbf{p} + \mathbf{q}} = -\mathbb{E}_{\xi \sim \mathbf{p}} \log \frac{1 + e^{\mu^\top \Sigma^{-1} \xi - \mu^\top \Sigma^{-1} \mu/2}}{2}$$

Let us introduce $\eta = \mu^\top \Sigma^{-1} \xi - \mu^\top \Sigma^{-1} \mu/2 \sim \mathcal{N}(-\mu^\top \Sigma^{-1} \mu/2, \mu^\top \Sigma^{-1} \mu)$. Since the second derivative of the map $u \mapsto \log((1 + e^u)/2)$ does not exceed $1/4$, Jensen's inequality implies that

$$\begin{aligned} \text{KL}\left(\mathbf{p}, \frac{\mathbf{p} + \mathbf{q}}{2}\right) &= -\mathbb{E} \ln \frac{1 + e^\eta}{2} \\ &\geq -\ln \frac{1 + e^{\mathbb{E}\eta}}{2} - \frac{\text{Var}(\eta)}{8} \\ &= -\ln \frac{1 + e^{-\mu^\top \Sigma^{-1} \mu/2}}{2} - \frac{\mu^\top \Sigma^{-1} \mu}{8}. \end{aligned}$$

Consider the function $g(u) = -\ln((1 + e^{-u})/2)$. Note that $g(0) = 0$, $g(1) > 1/3$, and g is concave on $[0, 1]$. This yields that $g(u) \geq u/3$ for all $u \in [0, 1]$. Hence,

$$\text{KL}\left(\mathbf{p}, \frac{\mathbf{p} + \mathbf{q}}{2}\right) \geq -\ln \frac{1 + e^{-\mu^\top \Sigma^{-1} \mu/2}}{2} - \frac{\mu^\top \Sigma^{-1} \mu}{8} \geq \frac{\mu^\top \Sigma^{-1} \mu}{6} - \frac{\mu^\top \Sigma^{-1} \mu}{8} = \frac{\mu^\top \Sigma^{-1} \mu}{24}.$$

Similarly, one can prove that

$$\text{KL}\left(\mathbf{q}, \frac{\mathbf{p} + \mathbf{q}}{2}\right) \gtrsim \mu^\top \Sigma^{-1} \mu,$$

and, therefore, $\text{JS}(\mathbf{p}, \mathbf{q}) \gtrsim \mu^\top \Sigma^{-1} \mu$.

VII. CONCLUSION AND FUTURE DIRECTIONS

We suggested novel online change point detection procedures which are suitable for both parametric and nonparametric scenarios. We derived high probability bounds on the running length and the detection delay of Algorithm II.1. As a consequence, we obtained the first non-asymptotic bound for online change point detection via neural networks. We also conducted numerical experiments on artificial and real-world data illustrating efficiency of the proposed methods.

Further research in this direction may include consideration of nonstationary post-change observations as in [37]. Besides, one may try to improve the dependence on B in the upper bound (7) using improper estimators instead of \hat{f} . In [17], the authors showed that a proper regularization leads to a doubly-exponential improvement in the dependence on B in the problem of logistic regression.

APPENDIX A

SOME PROPERTIES OF SUB-GAUSSIAN RANDOM VARIABLES

In this section, we provide some useful properties of sub-Gaussian random variables. For any random variable ξ , its Orlicz norm ψ_2 is defined as

$$\|\xi\|_{\psi_2} = \inf \left\{ t > 0 : \mathbb{E} e^{\xi^2/t^2} \leq 2 \right\}.$$

Random variables with a finite ψ_2 -norm are usually called sub-Gaussian, because the tails of their distributions decay as $O\left(e^{-t^2/\|\xi\|_{\psi_2}^2}\right)$. Indeed, by the definition of the Orlicz norm, we have

$$\mathbb{P}(|\xi| > t) \leq \frac{\mathbb{E} e^{|\xi|/\|\xi\|_{\psi_2}^2}}{e^{t^2/\|\xi\|_{\psi_2}^2}} \leq 2e^{-\frac{t^2}{\|\xi\|_{\psi_2}^2}}, \quad \text{for all } t > 0. \quad (20)$$

In its turn, the inequality (20) yields an upper bound on the L_p -norm of ξ . For any $p \geq 1$, it holds that

$$\begin{aligned} \mathbb{E}|\xi|^p &= \int_0^{+\infty} \mathbb{P}(|\xi|^p \geq u) du \leq 2 \int_0^{+\infty} e^{-u^{2/p}/\|\xi\|_{\psi_2}^2} du \\ &= p\|\xi\|_{\psi_2}^p \int_0^{+\infty} v^{p/2-1} e^{-v} dv = p\|\xi\|_{\psi_2}^p \Gamma\left(\frac{p}{2}\right) = 2\|\xi\|_{\psi_2}^p \Gamma\left(\frac{p}{2} + 1\right), \end{aligned} \quad (21)$$

where $\Gamma(\cdot)$ is the gamma function. There are several equivalent definitions of sub-Gaussian variables. A reader can find them, for instance, in [60, Proposition 2.5.2]. In our proofs, we deal with sums of independent sub-Gaussian random variables and use the following property.

Proposition A.1 ([60], Proposition 2.6.1). *Let ξ_1, \dots, ξ_n be independent centered sub-Gaussian random variables. Then their sum $S_n = \xi_1 + \dots + \xi_n$ is also sub-Gaussian, and its Orlicz norm satisfies the inequality*

$$\|S_n\|_{\psi_2}^2 \lesssim \sum_{i=1}^n \|\xi_i\|_{\psi_2}^2.$$

It is also worth mentioning that, according to [60, Lemma 2.6.8], the centering does not increase the ψ_2 -norm too much. That is, for any sub-Gaussian random variable ξ , it holds that

$$\|\xi - \mathbb{E}\xi\|_{\psi_2} \lesssim \|\xi\|_{\psi_2}. \quad (22)$$

APPENDIX B SOME PROPERTIES OF NEURAL NETWORKS

This section collects some useful properties of feed-forward neural networks with ReLU activations. Let us recall that $\text{NN}(L, \mathcal{A}, s)$ denotes the class of neural networks with L hidden layers, architecture \mathcal{A} , and at most s non-zero weights. The next theorem from [50] concerns approximation properties of neural networks.

Theorem B.1 ([50], Theorem 5). *For any $f^* \in \mathcal{H}^\beta([0, 1]^p, H)$ and any $N, m \in \mathbb{N}$, there exists a neural network $f \in \text{NN}(L, \mathcal{A}, s)$ with*

$$L = 8 + (m + 5)(1 + \lceil \log_2(p \vee \beta) \rceil)$$

hidden layers, the architecture

$$\mathcal{A} = (p, 6(\lceil \beta \rceil + p)N, \dots, 6(\lceil \beta \rceil + p)N, 1),$$

and the number of non-zero parameters

$$s \leq 141(p + \beta + 1)^{3+p}N(m + 6),$$

such that

$$\|f - f^*\|_{L_\infty([0, 1]^p)} \leq (1 + p^2 + \beta^2)6^p(2H + 1)N2^{-m} + 3^\beta HN^{-\beta/p}.$$

Taking a sufficiently deep and wide enough neural network, one can approximate any function from $\mathcal{H}^\beta([0, 1]^p, H)$ with the desired accuracy. On the other hand, Schmidt-Hieber established the following upper bound on the covering number of $\text{NN}(L, \mathcal{A}, s)$.

Lemma B.2 ([50], Lemma 5). *For any $L \in \mathbb{Z}_+$, $\mathcal{A} \in \mathbb{N}^{L+2}$, $s \in \mathbb{N}$, the covering number of the class $\text{NN}(L, \mathcal{A}, s)$ with respect to the $L_\infty([0, 1]^p)$ -norm satisfies the inequality*

$$\log \mathcal{N}(\text{NN}(L, \mathcal{A}, s), L_\infty([0, 1]^p), \varepsilon) \leq (s + 1) \log \left(\frac{2(L + 1)V^2}{\varepsilon} \right), \quad \text{for all } \varepsilon > 0,$$

where $V = \prod_{j=0}^{L+1} (1 + a_j)$.

APPENDIX C PROOF OF LEMMA VI.1

It holds that

$$-\mathbb{E}\mathcal{T}_{\tau, t}(f) = \frac{\tau(t - \tau)}{t} \mathbb{E} \left[-f(X_1) + 2 \ln \left(\frac{1 + e^{f(X_1)}}{2} \right) \right].$$

Consider a function $G : [-B, B] \rightarrow \mathbb{R}$, defined as

$$G(u) = -u + 2 \ln \left(\frac{1 + e^u}{2} \right).$$

Direct calculations show that $G(0) = G'(0) = 0$ and

$$G''(u) = \frac{2e^u}{(1 + e^u)^2} \geq 2\kappa, \quad \text{for all } u \in [-B, B],$$

where

$$\kappa = \min \left\{ \frac{e^B}{(1 + e^B)^2}, \frac{e^{-B}}{(1 + e^{-B})^2} \right\}.$$

Hence, using Taylor's expansion, we obtain that $G(u) \geq \varkappa u^2$ for all $u \in [-B, B]$. This yields that

$$\frac{\varkappa \tau(t-\tau) \mathbb{E} f^2(X_1)}{t} \leq -\mathbb{E} \mathcal{T}_{\tau,t}(f). \quad (23)$$

To prove the second part of the lemma, note that

$$\begin{aligned} \text{Var}(\mathcal{T}_{\tau,t}) &= \frac{\tau(t-\tau)^2}{t^2} \text{Var} \left[f(X_1) - \ln \left(\frac{1+e^{f(X_1)}}{2} \right) \right] + \frac{\tau^2(t-\tau)}{t^2} \text{Var} \left[\ln \left(\frac{1+e^{f(X_1)}}{2} \right) \right] \\ &\leq \frac{\tau(t-\tau)^2}{t^2} \mathbb{E} \left[f(X_1) - \ln \left(\frac{1+e^{f(X_1)}}{2} \right) \right]^2 + \frac{\tau^2(t-\tau)}{t^2} \mathbb{E} \left[\ln \left(\frac{1+e^{f(X_1)}}{2} \right) \right]^2. \end{aligned}$$

Since the functions $G_1(u) = u - \ln[(1+e^u)/2]$ and $G_2(u) = \ln[(1+e^u)/2]$ are 1-Lipschitz and $G_1(0) = G_2(0) = 0$, we have

$$\text{Var}(\mathcal{T}_{\tau,t}) \leq \frac{\tau(t-\tau)^2}{t^2} \mathbb{E} f^2(X_1) + \frac{\tau^2(t-\tau)}{t^2} \mathbb{E} f^2(X_1) = \frac{\tau(t-\tau)}{t} \mathbb{E} f^2(X_1) \leq \frac{-\mathbb{E} \mathcal{T}_{\tau,t}(f)}{\varkappa},$$

where the last inequality is due to (23).

APPENDIX D PROOF OF LEMMA VI.2

Let us recall that, for any $b \geq a > 0$, $\mathcal{F}(a, b)$ is defined as

$$\mathcal{F}(a, b) = \left\{ f \in \mathcal{F} : \frac{at}{\tau(t-\tau)} \leq \mathbb{E} f^2(X_1) \leq \frac{bt}{\tau(t-\tau)} \right\}.$$

Then it holds that

$$\begin{aligned} &\mathbb{E} \sup_{f \in \mathcal{F}} \left[4^{-k(f)} \mathcal{T}_{\tau,t}(f) - \mathbb{E} 4^{-k(f)} \mathcal{T}_{\tau,t}(f) \right] \\ &\leq \mathbb{E} \sup_{f \in \mathcal{F}(0,r)} \left[4^{-k(f)} \mathcal{T}_{\tau,t}(f) - \mathbb{E} 4^{-k(f)} \mathcal{T}_{\tau,t}(f) \right] \\ &\quad + \sum_{j=0}^{\infty} \mathbb{E} \sup_{f \in \mathcal{F}(4^j r, 4^{j+1} r)} \left[4^{-k(f)} \mathcal{T}_{\tau,t}(f) - \mathbb{E} 4^{-k(f)} \mathcal{T}_{\tau,t}(f) \right] \\ &\leq \mathbb{E} \sup_{f \in \mathcal{F}(0,r)} [\mathcal{T}_{\tau,t}(f) - \mathbb{E} \mathcal{T}_{\tau,t}(f)] + \sum_{j=0}^{\infty} 4^{-j} \mathbb{E} \sup_{f \in \mathcal{F}(0, 4^{j+1} r)} [\mathcal{T}_{\tau,t}(f) - \mathbb{E} \mathcal{T}_{\tau,t}(f)]. \end{aligned} \quad (24)$$

For any $f \in \mathcal{F}$, let us represent $\mathcal{T}_{\tau,t}(f)$ as a sum of two terms:

$$\mathcal{T}_{\tau,t}(f) = \frac{\tau(t-\tau)}{t} \mathcal{P}_{\tau,t}(f) + \frac{\tau(t-\tau)}{t} \mathcal{Q}_{\tau,t}(f),$$

where

$$\mathcal{P}_{\tau,t}(f) = \frac{1}{\tau} \sum_{s=1}^{\tau} \left[f(X_s) - \ln \left(\frac{1+e^{f(X_s)}}{2} \right) \right]$$

and

$$\mathcal{Q}_{\tau,t}(f) = -\frac{1}{t-\tau} \sum_{s=\tau+1}^t \ln \left(\frac{1+e^{f(X_s)}}{2} \right).$$

Then, for any $r > 0$, it holds that

$$\begin{aligned} \mathbb{E} \sup_{f \in \mathcal{F}(0,r)} [\mathcal{T}_{\tau,t}(f) - \mathbb{E} \mathcal{T}_{\tau,t}(f)] &\leq \frac{\tau(t-\tau)}{t} \mathbb{E} \sup_{f \in \mathcal{F}(0,r)} [\mathcal{P}_{\tau,t}(f) - \mathbb{E} \mathcal{P}_{\tau,t}(f)] \\ &\quad + \frac{\tau(t-\tau)}{t} \mathbb{E} \sup_{f \in \mathcal{F}(0,r)} [\mathcal{Q}_{\tau,t}(f) - \mathbb{E} \mathcal{Q}_{\tau,t}(f)]. \end{aligned}$$

We apply the following lemma to bound the expectations of the suprema in the right-hand side.

Lemma D.1 ([22], Lemma 7; in this form, [3], Lemma A.6). *Let ξ_1, \dots, ξ_n , $n \in \mathbb{N}$, be independent copies of a random variable $\xi \sim \mathbb{P}$, and let \mathcal{H} be a class of functions taking its values in $[-B, B]$. Suppose that, for all $0 < u \leq B$,*

$$\mathcal{N}_{[]}(\mathcal{H}, L_2(\mathbb{P}), u) \leq \left(\frac{A}{\varepsilon} \right)^d$$

for some positive constants A and d . Then

$$\mathbb{E} \sup_{h \in \mathcal{H}} \left[\frac{1}{n} \sum_{i=1}^n h(\xi_i) - \mathbb{E}h(\xi) \right] \lesssim \sqrt{\frac{d\sigma^2}{n} \log\left(\frac{A}{\sigma}\right)} + \frac{Bd}{n} \log\left(\frac{A}{\sigma}\right),$$

where $\sigma^2 = \sup_{h \in \mathcal{H}} \mathbb{E}h^2(\xi)$.

Note that the maps $y \mapsto (y - \log(1 + e^y))$ and $y \mapsto \log(1 + e^y)$ are monotonously increasing and 1-Lipschitz. This yields that if f belongs to a bracket $[f_1, f_2]$ of size ε , then $(f - \log(1 + e^f))$ is in the bracket $[f_1 - \log(1 + e^{f_1}), f_2 - \log(1 + e^{f_2})]$ of size at most ε and, similarly, $\log(1 + e^f)$ belongs to the bracket $[\log(1 + e^{f_1}), \log(1 + e^{f_2})]$ of size at most ε . In other words, a monotonous 1-Lipschitz map does not change the bracketing number. Thus, it holds that

$$\mathbb{E} \sup_{f \in \mathcal{F}(0,r)} [\mathcal{P}_{\tau,t}(f) - \mathbb{E}\mathcal{P}_{\tau,t}(f)] \lesssim \sqrt{\frac{rtd}{\tau^2(t-\tau)} \log\left(\frac{A\tau(t-\tau)}{rt}\right)} + \frac{Bd}{\tau} \log\left(\frac{A\tau(t-\tau)}{rt}\right)$$

and

$$\mathbb{E} \sup_{f \in \mathcal{F}(0,r)} [\mathcal{Q}_{\tau,t}(f) - \mathbb{E}\mathcal{Q}_{\tau,t}(f)] \lesssim \sqrt{\frac{rtd}{\tau(t-\tau)^2} \log\left(\frac{A\tau(t-\tau)}{rt}\right)} + \frac{Bd}{t-\tau} \log\left(\frac{A\tau(t-\tau)}{rt}\right).$$

Therefore, due to the definitions of $\mathcal{T}_{\tau,t}(f)$, $\mathcal{P}_{\tau,t}(f)$, and $\mathcal{Q}_{\tau,t}(f)$,

$$\begin{aligned} \mathbb{E} \sup_{f \in \mathcal{F}(0,r)} [\mathcal{T}_{\tau,t}(f) - \mathbb{E}\mathcal{T}_{\tau,t}(f)] &\lesssim \sqrt{\frac{rd(t-\tau)}{t} \log\left(\frac{A\tau(t-\tau)}{rt}\right)} + \sqrt{\frac{rd\tau}{t} \log\left(\frac{A\tau(t-\tau)}{rt}\right)} \\ &\quad + Bd \log\left(\frac{A\tau(t-\tau)}{rt}\right). \end{aligned}$$

Using the inequality $\sqrt{a} + \sqrt{b} \leq \sqrt{2(a+b)}$, which holds for all non-negative a and b , we obtain that

$$\mathbb{E} \sup_{f \in \mathcal{F}(0,r)} [\mathcal{T}_{\tau,t}(f) - \mathbb{E}\mathcal{T}_{\tau,t}(f)] \lesssim \sqrt{rd \log\left(\frac{A\tau(t-\tau)}{rt}\right)} + Bd \log\left(\frac{A\tau(t-\tau)}{rt}\right). \quad (25)$$

Similarly, we can prove that

$$\begin{aligned} \mathbb{E} \sup_{f \in \mathcal{F}(0,4^{j+1}r)} [\mathcal{T}_{\tau,t}(f) - \mathbb{E}\mathcal{T}_{\tau,t}(f)] &\lesssim \sqrt{4^{j+1}rd \log\left(\frac{A\tau(t-\tau)}{4^{j+1}rt}\right)} \\ &\quad + Bd \log\left(\frac{A\tau(t-\tau)}{4^{j+1}rt}\right). \end{aligned} \quad (26)$$

Substituting the bounds (25) and (26) into the inequality (24), we get that

$$\begin{aligned} \mathbb{E} \sup_{f \in \mathcal{F}} [\mathcal{T}_{\tau,t}(f) - \mathbb{E}\mathcal{T}_{\tau,t}(f)] &\lesssim \sum_{j=0}^{\infty} 4^{-j} \left[\sqrt{4^j rd \log\left(\frac{A\tau(t-\tau)}{4^j rt}\right)} + Bd \log\left(\frac{A\tau(t-\tau)}{4^j rt}\right) \right] \\ &\lesssim \sqrt{rd \log\left(\frac{A\tau(t-\tau)}{rt}\right)} + Bd \log\left(\frac{A\tau(t-\tau)}{rt}\right). \end{aligned}$$

APPENDIX E PROOF OF LEMMA VI.3

Similarly to Lemma VI.1, we have

$$-\mathbb{E}\mathcal{T}_{\tau,t}(f) = \frac{\tau(t-\tau)}{t} \mathbb{E} \left[-f(X_1) + 2 \ln \left(\frac{1 + e^{f(X_1)}}{2} \right) \right].$$

Consider a function $G : \mathbb{R} \rightarrow \mathbb{R}$, defined as

$$G(u) = -u + 2 \ln \left(\frac{1 + e^u}{2} \right).$$

Direct calculations show that $G(0) = G'(0) = 0$ and

$$G''(u) = \frac{2e^u}{(1+e^u)^2} \geq \frac{e^u}{2(1 \vee e^u)^2} = \frac{e^u \wedge e^{-u}}{2} = \frac{e^{-|u|}}{2}.$$

Using Taylor's expansion with an integral remainder, we obtain that

$$G(u) \geq u^2 \int_0^1 G''(yu)(1-y)dy \geq \frac{u^2}{2} \int_0^1 e^{-y|u|}(1-y)dy \geq \frac{u^2 e^{-|u|}}{4}.$$

This yields

$$\mathbb{E} \left[-f(X_1) + 2 \ln \left(\frac{1 + e^{f(X_1)}}{2} \right) \right] \geq \frac{\mathbb{E} f^2(X_1) e^{-|f(X_1)|}}{4}.$$

Denote $\xi = |f(X_1)|$ and note that $\|\xi\|_{\psi_2} = \|f(X_1)\|_{\psi_2}$. Then it holds that

$$\mathbb{E} [\xi^2 e^{-\xi}] \geq \mathbb{E} [\xi^2 e^{-\xi} \mathbb{I}(\xi \leq a)] \geq e^{-a} \mathbb{E} [\xi^2 \mathbb{I}(\xi \leq a)] = e^{-a} \mathbb{E} \xi^2 - e^{-a} \mathbb{E} [\xi^2 \mathbb{I}(\xi > a)].$$

Consider the second term in the right-hand side. Due to the Cauchy-Schwarz inequality, it holds that

$$\mathbb{E} [\xi^2 \mathbb{I}(\xi > a)] \leq \sqrt{\mathbb{E} \xi^4 \mathbb{P}(\xi > a)}.$$

Applying the inequality (21) for L_p -norms of sub-Gaussian random variables, we obtain that $\mathbb{E} \xi^4 \leq 4 \|\xi\|_{\psi_2}^4$ and, thus,

$$\mathbb{E} [\xi^2 \mathbb{I}(\xi > a)] \leq 2\sqrt{2} \|\xi\|_{\psi_2}^2 \exp \left\{ -\frac{a^2}{2 \|\xi\|_{\psi_2}^2} \right\}.$$

Taking $a = \|\xi\|_{\psi_2} \sqrt{2 \ln(4L\sqrt{2})}$, we finally obtain that

$$\mathbb{E} [\xi^2 \mathbb{I}(\xi > a)] \leq \frac{\|\xi\|_{\psi_2}}{L} \leq \mathbb{E} \xi^2,$$

where the last inequality is due to the sub-Gaussianity of the class \mathcal{F} . Hence,

$$\mathbb{E} [\xi^2 e^{-\xi}] \geq \frac{e^{-a}}{2} \mathbb{E} \xi^2 = \frac{\mathbb{E} \xi^2}{2} \exp \left\{ -\|\xi\|_{\psi_2} \sqrt{2 \ln(4L\sqrt{2})} \right\} = \kappa_\xi \mathbb{E} \xi^2,$$

where we introduced

$$\kappa_\xi = \frac{1}{2} \exp \left\{ -\|\xi\|_{\psi_2} \sqrt{2 \ln(4L\sqrt{2})} \right\}.$$

In other words, for any $f \in \mathcal{F}$, it holds that

$$\kappa_{f(X_1)} \mathbb{E} f^2(X_1) \leq \mathbb{E} f^2(X_1) e^{-|f(X_1)|} \leq \mathbb{E} \left[-f(X_1) + 2 \ln \left(\frac{1 + e^{f(X_1)}}{2} \right) \right] = -\frac{\tau(t-\tau)}{t} \mathbb{E} \mathcal{T}_{\tau,t}(f).$$

This yields the desired result.

REFERENCES

- [1] S. Arlot, A. Celisse, and Z. Harchaoui, "A kernel multiple change-point algorithm via model selection," *Journal of Machine Learning Research*, vol. 20, no. 162, pp. 1–56, 2019.
- [2] P. L. Bartlett, O. Bousquet, and S. Mendelson, "Local Rademacher complexities," *The Annals of Statistics*, vol. 33, no. 4, pp. 1497–1537, 2005.
- [3] D. Belomestny, L. Iosipoi, Q. Paris, and N. Zhivotovskiy, "Empirical variance minimization with applications in variance reduction and optimal control," *Bernoulli*, vol. 28, no. 2, pp. 1382–1407, 2022.
- [4] G. Biau, K. Bleakley, and D. M. Mason, "Long signal change-point detection," *Electronic Journal of Statistics*, vol. 10, no. 2, pp. 2097–2123, 2016.
- [5] Y. Cao, L. Xie, Y. Xie, and H. Xu, "Sequential change-point detection via online convex optimization," *Entropy*, vol. 20, no. 2, p. 108, 2018.
- [6] W.-C. Chang, C.-L. Li, Y. Yang, and B. Póczos, "Kernel change-point detection with auxiliary deep generative models," in *International Conference on Learning Representations*, 2019.
- [7] Y. Chen, T. Wang, and R. J. Samworth, "High-dimensional, multiscale online changepoint detection," *Journal of the Royal Statistical Society: Series B (Statistical Methodology)*, vol. 84, pp. 234–266, 2022.
- [8] L. Chu and H. Chen, "Sequential change-point detection for high-dimensional and non-euclidean data," *IEEE Transactions on Signal Processing*, vol. 70, pp. 4498–4511, 2022.
- [9] R. Corradin, L. Danese, and A. Ongaro, "Bayesian nonparametric change point detection for multivariate time series with missing observations," *International Journal of Approximate Reasoning*, vol. 143, pp. 26–43, 2022.
- [10] R. C. Dalang and A. N. Shiryaev, "A quickest detection problem with an observation cost," *The Annals of Applied Probability*, vol. 25, no. 3, pp. 1475–1512, 2015.

- [11] H. Dehling, K. Vuk, and M. Wendler, “Change-point detection based on weighted two-sample U-statistics,” *Electronic Journal of Statistics*, vol. 16, no. 1, pp. 862–891, 2022.
- [12] H. Dette and J. Gösmann, “A likelihood ratio approach to sequential change point detection for a general class of parameters,” *Journal of the American Statistical Association*, vol. 115, no. 531, pp. 1361–1377, 2020.
- [13] L. Dümbgen and V. G. Spokoiny, “Multiscale testing of qualitative hypotheses,” *The Annals of Statistics*, vol. 29, no. 1, pp. 124–152, 2001.
- [14] B. Eichinger and C. Kirch, “A MOSUM procedure for the estimation of multiple random change points,” *Bernoulli*, vol. 24, no. 1, pp. 526–564, 2018.
- [15] F. Enikeeva and Z. Harchaoui, “High-dimensional change-point detection under sparse alternatives,” *The Annals of Statistics*, vol. 47, no. 4, pp. 2051–2079, 2019.
- [16] A. Ferrari, C. Richard, A. Bourrier, and I. Bouchikhi, “Online change-point detection with kernels,” *Pattern Recognition*, vol. 133, p. 109022, 2023.
- [17] D. J. Foster, S. Kale, H. Luo, M. Mohri, and K. Sridharan, “Logistic regression: The importance of being improper,” in *Proceedings of the 31st Conference On Learning Theory*, ser. Proceedings of Machine Learning Research, vol. 75, 2018, pp. 167–208.
- [18] D. Garreau and S. Arlot, “Consistent change-point detection with kernels,” *Electronic Journal of Statistics*, vol. 12, no. 2, pp. 4440–4486, 2018.
- [19] I. Goodfellow, J. Pouget-Abadie, M. Mirza, B. Xu, D. Warde-Farley, S. Ozair, A. Courville, and Y. Bengio, “Generative adversarial nets,” in *Advances in neural information processing systems*, 2014, pp. 2672–2680.
- [20] A. Grover, J. Song, A. Kapoor, K. Tran, A. Agarwal, E. J. Horvitz, and S. Ermon, “Bias correction of learned generative models using likelihood-free importance weighting,” in *Advances in Neural Information Processing Systems*, vol. 32, 2019.
- [21] M. U. Gutmann and A. Hyvärinen, “Noise-contrastive estimation of unnormalized statistical models, with applications to natural image statistics,” *Journal of Machine Learning Research*, vol. 13, pp. 307–361, 2012.
- [22] Q. Han, T. Wang, S. Chatterjee, and R. J. Samworth, “Isotonic regression in general dimensions,” *The Annals of Statistics*, vol. 47, no. 5, pp. 2440–2471, 2019.
- [23] Z. Harchaoui, E. Moulines, and F. Bach, “Kernel change-point analysis,” in *Advances in Neural Information Processing Systems*, vol. 21, 2008.
- [24] T. Hastie, R. Tibshirani, and J. Friedman, *The elements of statistical learning*, 2nd ed., ser. Springer Series in Statistics. Springer, New York, 2009, data mining, inference, and prediction.
- [25] E. Hazan, “Introduction to online convex optimization,” *Foundations and Trends® in Optimization*, vol. 2, no. 3-4, pp. 157–325, 2016.
- [26] E. Hazan, A. Agarwal, and S. Kale, “Logarithmic regret algorithms for online convex optimization,” *Machine Learning*, vol. 69, no. 2, pp. 169–192, 2007.
- [27] A. Hero, “Geometric entropy minimization (gem) for anomaly detection and localization,” in *Advances in Neural Information Processing Systems*, vol. 19, 2006.
- [28] M. Hushchyn and A. Ustyuzhanin, “Generalization of change-point detection in time series data based on direct density ratio estimation,” *J. Comput. Sci.*, vol. 53, pp. Paper No. 101 385, 8, 2021.
- [29] M. Hushchyn, K. Arzimatov, and D. Derkach, “Online neural networks for change-point detection,” Preprint, arXiv:2010.01388, 2020.
- [30] T. Kanamori, S. Hido, and M. Sugiyama, “A least-squares approach to direct importance estimation,” *Journal of Machine Learning Research*, vol. 10, pp. 1391–1445, 2009.
- [31] D. P. Kingma and J. Ba, “Adam: A method for stochastic optimization,” in *3rd International Conference for Learning Representations*, 2015.
- [32] T. Klein and E. Rio, “Concentration around the mean for maxima of empirical processes,” *The Annals of Probability*, vol. 33, no. 3, pp. 1060–1077, 2005.
- [33] K. K. Korkas and P. Fryzlewicz, “Multiple change-point detection for non-stationary time series using wild binary segmentation,” *Statistica Sinica*, vol. 27, no. 1, pp. 287–311, 2017.
- [34] M. N. Kurt, Y. Yilmaz, and X. Wang, “Real-time nonparametric anomaly detection in high-dimensional settings,” *IEEE Transactions on Pattern Analysis and Machine Intelligence*, vol. 43, pp. 2463–2479, 2021.
- [35] M. Ledoux and M. Talagrand, *Probability in Banach spaces. Isoperimetry and processes*, reprint of the 1991 ed. Berlin: Springer, 2011.
- [36] S. Li, Y. Xie, H. Dai, and L. Song, “M-statistic for kernel change-point detection,” in *Advances in Neural Information Processing Systems*, vol. 28, 2015.
- [37] Y. Liang, A. G. Tartakovsky, and V. V. Veeravalli, “Quickest change detection with non-stationary post-change observations,” Preprint, arXiv:2110.01581, 2021.
- [38] S. Liu, M. Yamada, N. Collier, and M. Sugiyama, “Change-point detection in time-series data by relative density-ratio estimation,” *Neural Networks*, vol. 43, pp. 72–83, 2013.

- [39] M. Londschien, P. Bühlmann, and S. Kovács, “Random forests for change point detection,” *Journal of Machine Learning Research*, vol. 24, no. 216, pp. 1–45, 2023.
- [40] O. H. Madrid Padilla, Y. Yu, D. Wang, and A. Rinaldo, “Optimal nonparametric change point analysis,” *Electronic Journal of Statistics*, vol. 15, no. 1, pp. 1154–1201, 2021.
- [41] —, “Optimal nonparametric multivariate change point detection and localization,” *IEEE Transactions on Information Theory*, vol. 68, no. 3, pp. 1922–1944, 2022.
- [42] D. S. Matteson and N. A. James, “A nonparametric approach for multiple change point analysis of multivariate data,” *Journal of the American Statistical Association*, vol. 109, no. 505, pp. 334–345, 2014.
- [43] E. S. Page, “Continuous inspection schemes,” *Biometrika*, vol. 41, no. 1-2, pp. 100–115, 06 1954.
- [44] —, “A test for a change in a parameter occurring at an unknown point,” *Biometrika*, vol. 42, no. 3-4, pp. 523–527, 12 1955.
- [45] F. Pein, H. Sieling, and A. Munk, “Heterogeneous change point inference,” *Journal of the Royal Statistical Society. Series B. Statistical Methodology*, vol. 79, no. 4, pp. 1207–1227, 2017.
- [46] M. Pollak and A. G. Tartakovsky, “Optimality properties of the Shiryaev-Roberts procedure,” *Statistica Sinica*, vol. 19, no. 4, pp. 1729–1739, 2009.
- [47] N. Puchkin and V. Shcherbakova, “A contrastive approach to online change point detection,” in *Proceedings of The 26th International Conference on Artificial Intelligence and Statistics*, ser. Proceedings of Machine Learning Research, vol. 206. PMLR, 2023, pp. 5686–5713.
- [48] A. Rinaldo, D. Wang, Q. Wen, R. Willett, and Y. Yu, “Localizing changes in high-dimensional regression models,” in *Proceedings of The 24th International Conference on Artificial Intelligence and Statistics*, ser. Proceedings of Machine Learning Research, vol. 130, 2021, pp. 2089–2097.
- [49] S. W. Roberts, “A comparison of some control chart procedures,” *Technometrics*, vol. 8, no. 3, pp. 411–430, 1966.
- [50] J. Schmidt-Hieber, “Nonparametric regression using deep neural networks with relu activation function,” *Annals of Statistics*, vol. 48, no. 4, pp. 1875–1897, 2020.
- [51] S. Shalev-Shwartz, “Online learning and online convex optimization,” *Foundations and Trends® in Machine Learning*, vol. 4, no. 2, pp. 107–194, 2012.
- [52] J. Shin, A. Ramdas, and A. Rinaldo, “E-detectors: a nonparametric framework for online changepoint detection,” Preprint, arXiv:2203.03532, 2022.
- [53] A. N. Shiryaev, “The problem of the most rapid detection of a disturbance in a stationary process,” *Soviet Mathematics. Doklady*, vol. 2, pp. 795–799, 1961.
- [54] —, “On optimum methods in quickest detection problems,” *Theory of Probability and its Applications*, vol. 8, pp. 22–46, 1963.
- [55] M. Sugiyama, T. Suzuki, S. Nakajima, H. Kashima, P. von Bünau, and M. Kawanabe, “Direct importance estimation for covariate shift adaptation,” *Annals of the Institute of Statistical Mathematics*, vol. 60, no. 4, pp. 699–746, 2008.
- [56] Y.-W. Sun, K. Papagiannouli, and V. Spokoiny, “High dimensional change-point detection: a complete graph approach,” Preprint, arXiv:2203.08709, 2022.
- [57] A. G. Tartakovsky, M. Pollak, and A. S. Polunchenko, “Third-order asymptotic optimality of the generalized shiryaev-roberts changepoint detection procedures,” *Theory of Probability & Its Applications*, vol. 56, no. 3, pp. 457–484, 2012.
- [58] M. K. Titsias, J. Sygnowski, and Y. Chen, “Sequential changepoint detection in neural networks with checkpoints,” *Statistics and Computing*, vol. 32, no. 2, p. 26, 2022.
- [59] G. J. J. van den Burg and C. K. I. Williams, “An evaluation of change point detection algorithms,” 2022.
- [60] R. Vershynin, *High-Dimensional Probability: An Introduction with Applications in Data Science*. Cambridge University Press, 2018.
- [61] D. Wang, Y. Yu, and A. Rinaldo, “Univariate mean change point detection: penalization, CUSUM and optimality,” *Electronic Journal of Statistics*, vol. 14, no. 1, pp. 1917–1961, 2020.
- [62] G. M. Weiss, K. Yoneda, and T. Hayajneh, “Smartphone and smartwatch-based biometrics using activities of daily living,” *IEEE Access*, vol. 7, pp. 133 190–133 202, 2019.
- [63] M. Yamada, T. Suzuki, T. Kanamori, H. Hachiya, and M. Sugiyama, “Relative density-ratio estimation for robust distribution comparison,” *Neural Computation*, vol. 25, no. 5, pp. 1324–1370, 2013.
- [64] Y. Yu, S. Chatterjee, and H. Xu, “Localising change points in piecewise polynomials of general degrees,” Preprint, arXiv:2007.09910, 2020.
- [65] Y. Yu, O. H. M. Padilla, D. Wang, and A. Rinaldo, “A note on online change point detection,” Preprint, arXiv:2006.03283, 2020.
- [66] C. Zou, G. Yin, L. Feng, and Z. Wang, “Nonparametric maximum likelihood approach to multiple change-point problems,” *The Annals of Statistics*, vol. 42, no. 3, pp. 970–1002, 2014.